- A direct linear relationship was found between the pore volume and the size of the aromatic cluster of the coke. Also, an indirect linear relationship was observed between the amount of coating material and the number of aromatic carbons per aromatic cluster.

- Only about 13% of the aromatic carbons in Illinois No. 6 coal was hydrogenated during UOP bench-scale coprocessing with Lloydminster vacuum residue. Almost two-thirds of the aromatic carbons in Black Thunder subbituminous coal was hydrogenated during Wilsonville two-stage processing.

- Gas production accounted for 90% of the hydrogen consumed during UOP bench-scale coprocessing. For Wilsonville, Run 263, most of the hydrogen consumed in the first stage for periods G and J involved heteroatom reactions. During second stage processing, 46.3 moles of hydrogen were consumed during period J, while 20.7 were consumed during period G. This was attributed to the addition of catalyst Criterion 324 whose effect was to increase the slurry throughput during period J. For the overall process, the major differences in the hydrogen consuming reactions between the two periods involved matrix cleavage and heteroatomic gas reactions.

Related Publications

Guffey, F.D., D.A. Netzel, F.P. Miknis, and K.P. Thomas, 1993, Investigations into Coal Coprocessing and Coal Liquefaction. Laramie, WY, WRI-93-R018.

Netzel, D.A., F.P. Miknis, T. Zhang, P.D. Jacobs, H.W. Haynes, Jr., 1994, Carbon-13 Solid State NMR Structural Investigation of Coke Deposits on Spent Catalysts Used in Coal Liquefaction. Journal article in preparation.

VALUE-ADDED COAL PRODUCTS

Norman W. Merriam

Background

It is relatively easy to develop a process to drive the moisture from Powder River Basin (PRB) coal. A large number of combinations of gas flow and temperature can be used to dry minus 8-mesh PRB coal to zero or low moisture content using a fluidized-bed having a coal residence time of 3 minutes. However, the dried coal must be stabilized to maintain the characteristics of a good-quality fuel.

A premium-quality fuel process should go beyond simply removing water from coal. Much of the oxygen in PRB coal can be removed by driving carbon dioxide, and some carbon monoxide, from the coal. This partial decarboxylation not only increases the heating value of the coal, but the removal of oxygen from the coal helps to stabilize the coal and to reduce the susceptibility to self-heating. Partial decarboxylation was controlled in previous mild-gasification work to avoid generation of coal liquid in the dryer. In the reactor used, tar was driven from the coal at temperatures above 315°C (600°F).

Objectives

Western Research Institute is developing a process to produce a premium-quality, solid fuel from low-rank coal. This process is based upon past experience with development of coal-drying and mild-gasification processes and what has been learned from technical and economic evaluation of those processes. The process, called COMPCOAL™, focuses on a low-cost method to produce a premium-quality fuel that is less susceptible to formation of dust, reabsorption of moisture, and self-heating than the parent coal. The COMPCOAL product must also have a high heating value, as well as low sulfur and moisture content, and must exhibit good combustion characteristics.

Procedures

An existing bench-scale inclined fluidized-bed (IFB) reactor system was modified by adding a stabilizer into the effluent gas line. The stabilizer is a batch fluidized-bed reactor that was loaded with char or raw coal before the start of a test. Carbon dioxide was passed through the system, the IFB reactor was heated to the test temperature, and minus 16-mesh Wyodak coal was fed to the IFB reactor at a rate of 10 lb/hr for a period of either 0.25 or 0.50 hour. The high-boiling fraction of the pyrolysis liquids (pitch) was deposited on the char or coal in the stabilizer. The low-boiling fraction of the coal liquid passed through the stabilizer because the stabilizer was maintained at a temperature above the dew point of this fraction.

To evaluate the economics of the process, the cost of capital equipment items were proportioned from published costs of similar equipment designed for a 1000-ton-per-day (TPD) mild-gasification plant using PRB coal. It was assumed that the plant would be located at a PRB mine and would use existing crushing and screening equipment. The plant would operate for 300 days each year and produce 573 TPD of COMPCOAL product. The plant would use 16.6×10^9 Btu/day in coal feed in producing 14.3×10^9 Btu/day of COMPCOAL, for a conversion efficiency of 86%.

PRB coal was charged to the operating costs at a rate of $4.25/ton. A 10-year straight-line depreciation was used to provide rapid recovery of the capital investment and to simplify the calculations. Electrical power was estimated by proportioning gas flow rates to horsepower taken from a preliminary design. Fifty percent debt financing was assumed for the project.

Results

In the process, char containing 20 to 25 wt % volatiles and having a gross heating value of 12,500 to 13,000 Btu/lb is produced. The char is then contacted by smoke, driven from the char, depositing 6 to 8 wt % pitch on the char particles. Gas and vapors not deposited on the char are burned as fuel.

The economic evaluation shows the process will be economically attractive if the product can be sold for about $20/ton or more.

Conclusions

Preliminary tests show that pitch can be deposited on char, resulting in a product that is less dusty and less susceptible to reabsorption of moisture than raw PRB coal. Initial evaluation indicates that additional development of the COMPCOAL process is justified.

Related Publication

Merriam, N.W., and V.K. Sethi, 1992, Initial Evaluation of a Process for the Production of a Premium, Solid Fuel from Powder River Basin Coal. Laramie, WY, WRI-92-R004.

COAL REFERENCES

Anderson, R., E.N. Givens, and F. Derbyshire, 1993, Assessment of Small Particle Iron Oxide Catalysts for Coal Liquefaction. Amer. Chem. Soc. Div. Fuel Chem., 38(2): 495-502.

Berkowitz, N., and J.G. Speight, 1973, Prevention of "Spontaneous Heating" by Low-Temperature Immersion Carbonization of Coal. The Canadian Mining and Metallurgical Bulletin, August 1973.

Boysen, J.E., C.Y. Cha, F.A. Barbour, T.F. Turner, T.W. Kang, M.H. Berggren, R.F. Hogsett, and M.C. Jha, 1990, Development of an Advanced Process for Drying Fine Coal in an Inclined Fluidized Bed, Final Report. Laramie, WY, DOE/PC/88886-T5.

Ceylan, K. and L.M. Stock, 1991, Reaction Pathways during Coprocessing. Reaction of Illinois #6 and Wyodak Coals with Lloydminster and Hondo Residua under Mild Conditions. Energy and Fuels, 5: 482-487.

Derbyshire, F., A. Davis, M. Epstein, and P. Stansberry, 1986, Temperature-Staged Catalytic Coal Liquefaction. Fuel, 65: 1233-1239.

Derbyshire, F., A. Davis, H. Schobert, and P. Stansberry, 1990, Low-Temperature Catalytic Coal Hydrogenation: Pretreatment for Liquefaction. ACS Div. Fuel Chem., 199th National Meeting, Boston, MA, April 22-27, p. 51-57.

Finseth, D., D.L. Cillo, R.F. Sprecher, H.L. Retcofsky, and R.G. Lett, 1985, Changes in Hydrogen Utilization with Temperature During Direct Coal Liquefaction. Fuel, 64: 1718.

Guffey, F.D., F.A. Barbour, and R.F. Blake, 1992, Induced Coal Swelling and Co-Processing with a Mild-Gasification Produced Liquid. Fuel Sci. and Tech. Int., 10: 1207-1232.

Guffey, F.D., D.A. Netzel, F.P. Miknis, and K.P. Thomas, 1993, Investigations into Coal Coprocessing and Coal Liquefaction. Laramie, WY, WRI-93-R018.

Hayashi, S., and K. Hayamizu, 1989, Shift References in High-Resolution Solid-State NMR. Bull. Chem. Soc. Jpn., 62: 2429-2430.

Joseph, J.T., 1991, Liquefaction Behavior of Solvent-Swollen Coals. Fuel, 70: 139-144.

Kamiya, Y., T. Nobusawa and, S. Futamura, 1988, Catalytic Effects of Iron Compounds and the Role of Sulfur in Coal Liquefaction and Hydrogenolysis of SRC. Fuel Processing Technology, 18: 1-10.

McMillen, D.F., R. Malhotra, and D.S Tse, 1991, Interactive Effects Between Solvent Components: Possible Chemical Origin of Synergy in Liquefaction and Coprocessing. Energy and Fuels, 5: 179-187.

Merriam, N.W., and M.C. Jha, 1991, Final Report - Development of an Advanced, Continuous Mild-Gasification Process for the Production of Co-Products. Laramie, WY, WRI-91-R068.

Merriam, N.W., C.Y. Cha, T.W. Kang, and M.B. Vaillancourt, 1990, Development of an Advanced, Continuous Mild-Gasification Process for the Production of Coproducts, Topical Report for Task 4, Mild Gasification Tests--System Integration Studies. Laramie, WY, WRI-91-R023.

Miknis, F.P., D.A. Netzel, S.D. Brandes, R.A. Winschel, and F.P. Burke, 1993, NMR Determination of Aromatic Carbon Balances and Hydrogen Utilization in Direct Coal Liquefaction. Fuel, 72: 217-224.

Netzel, D.A., F.P. Miknis, T. Zhang, P.D. Jacobs, H.W. Haynes, Jr., 1994, Carbon-13 Solid State NMR Structural Investigation of Coke Deposits on Spent Catalysts Used in Coal Liquefaction. Journal article in preparation.

Piasecki, C.A., J.G. Gatsis, and H.E. Fullerton, 1991, UOP Slurry-Catalyzed Co-Processing. Proceedings Liquefaction Contractor's Review Meeting, G.J. Stigel, ed., Pittsburgh Energy Technology Center, Pittsburgh, PA, 598-615.

Solum, M.S., R.J. Pugmire, and D.M. Grant, 1989, ^{13}C Solid-State NMR of Argonne Premium Coals. Energy & Fuels, 3: 187-193.

Speight, J.G and S.E. Moschopedis, 1986, The Co-Processing of Coal with Heavy Feedstocks. Fuel Processing Technology, 13: 215-221.

Vaillancourt, M., T.F. Turner, and L.J. Fahy, 1991, Initial Study of Coal Pretreatment and Co-Processing. Laramie, WY, WRI-92-R002.

Warzinski, R., 1990, Catalyst Dispersion and Reagent Penetration. Proceedings Direct Liquefaction Contractor's Review Meeting, Pittsburgh, PA, p. 320-336.

Watanabe, Y., O. Yamada, K. Fujita, Y. Takegami, and T. Suzuki, 1984, Coal Liquefaction Using Iron Complexes as Catalysts. Fuel, 63: 752-755.

Zhang, T., 1993, Ph.D. Thesis, Department of Chemical Engineering, University of Wyoming.

ADVANCED EXPLORATORY

PROCESS TECHNOLOGY

THE USE OF OIL SHALE AS A SULFUR SORBENT IN A CIRCULATING FLUIDIZED-BED COMBUSTOR

John S. Nordin

Background

The use of limestone or dolomite as a sulfur sorbent in fluidized-bed combustion of coal was reviewed by Nordin and Cha (1989). They found that, typically, pilot circulating fluidized-bed combustors achieved a 90% reduction in sulfur emissions using a limestone calcium to coal sulfur ratio of 2.3 to 2.7, expressed as a molar ratio of Ca:S. With bubbling fluidized beds the molar ratio of Ca:S ranged from 2.9 to 3.5. When lower-sulfur coal was combusted, much higher ratios of Ca:S were required to achieve a 90% reduction in sulfur emissions. The optimal capture of sulfur on limestone was achieved at temperatures of 815 to 870°C (1500 to 1600°F), with sulfur capture significantly decreasing at temperatures above 900°C (1652°F). The Ca:S ratio required for a 90% sulfur emissions reduction was lower for dolomite than conventional limestone, especially in pressurized fluidized-bed combustors, with a Ca:S ratio of 1.4 being typical for a dolomite containing 45% $MgCO_3$. The magnesium carbonate was believed to be converted to magnesium oxide in the fluidized-bed combustor, resulting in a much more porous structure for sorbing sulfur gases.

Oil shale should theoretically offer a much more favorable Ca:S ratio compared to limestone when used as a sulfur sorbent in coal-fired fluidized-bed combustors. The surface area of retorted or combusted oil shale exposed to sulfur gases from coal should be large compared to limestone; not just because of the magnesium carbonate content, but also because of voids left by the kerogen. In addition, raw oil shale has a heating value, typically ranging from 1100 to 3400 Btu/lb, compared to zero for limestone. These advantages should be expected to be partially offset by the higher ash content of combusted oil shale.

This study was done in 1989 when the old Clean Air Act rules were in effect. Those rules required a 90% reduction in sulfur emissions for electric utility steam generators burning solid fuels and constructed after September 18, 1978 if the potential to emit without controls was equal to or greater than 0.60 lb of sulfur dioxide per million Btu heat input. If the potential to emit was less than 0.60 lb of sulfur per million Btu heat input, a 70% reduction was required. This meant that the utility must achieve at least an additional 70% reduction in sulfur, even when burning low-sulfur coals. The Clean Air Act of 1990 removed the restriction that another 70 or 90% reduction in sulfur emissions must be removed, regardless of the sulfur content of the coal.

Objective

The objective of this study was to perform a technical and economic assessment of using oil shale as a sulfur sorbent with three western coals in a circulating fluidized-bed combustion power plant, such as the one being tested in Nucla, Colorado.

Procedures

The study approach was to evaluate the operating experience of Colorado-Ute Electric Association's circulating fluidized-bed power plant in Nucla, Colorado, through 1989. This facility completed a series of tests using limestone as a sulfur sorbent for three western coals. The Nucla power plant conditions were then extrapolated for oil shale in place of limestone based on pilot plant tests performed by Synfuels Engineering and Development Inc. (1988), who evaluated sulfur removal using limestone, spent oil shale, and raw oil shale. Additional research work, reviewed by Cha and Fahy (1989), was incorporated into this study, as well as input from Pyropower Corporation,

which provided the Nucla power plant circulating fluidized-bed combustor. The Nucla power plant tests were funded in part by the Electric Power Research Institute, which provided results of some of the facility tests (Friedman et al. 1989).

An economic comparison was then made between limestone and three raw and one combusted oil shale as sulfur sorbents for three western coals under conditions similar to those experienced at the Nucla power plant. The three western coals evaluated were Peabody A (0.73% S, 26.1% ash, 5.8% water), Peabody B (2.5% S, 33% ash, 6.0% water), and Salt Creek (0.44% S, 15.1% ash, 9.9% water). The limestone used as a base comparison cost the Nucla power plant $20.90 per ton, delivered, and contained approximately 90% calcium carbonate, 1.8% magnesium carbonate, and 8.2 % silica and other impurities. The hypothetical oil shales used for the economic comparison had properties as listed in Table 1. When computing limestone or oil shale sorbent requirements, the assumption was made that the Nucla power plant must meet either a 70% reduction in sulfur emissions or the Colorado emission standard of 0.4 lb sulfur dioxide per million Btu input, whichever was more stringent. These were the emission limits imposed on the power plant in 1989. The Colorado standard was the limiting condition for the Peabody coal, but the federal 70% reduction was the limiting condition for the Salt Creek coal.

Results

An average Ca:S molar ratio was calculated for the three coals used at the Nucla power plant using limestone from plant data. If the calcium included the calcium in the limestone plus the calcium in the coal, the molar ratios required to meet emission standards were 1.76, 3.44, and 2.1 for Peabody A, Peabody B, and Salt Creek coals, respectively. These numbers compare with values of 1.61, 3.50, and 1.32 for the respective coals using limestone based on extrapolation of Synfuels Engineering and Development (1988) data. On this basis, the molar alkali to sulfur ratio for oil shale for the three respective coals should be 0.77, 2.75, and 0.5 at 871°C (1600°F). When doing the economic analysis for oil shale, an alkali to sulfur molar ratio of 1.0 rather than 0.5 was assumed for Salt Creek coal. When limestone was used with Salt Creek coal, a 1.32 molar ratio was predicted, compared to the 2.1 molar ratio actually experienced. Agreement between Nucla power plant data and extrapolated data for Peabody coal was very good.

Table 1. Oil Shale Compositions Used in Economic Analysis

	Combusted Shale	Retorted Shale	Low-Grade Shale	Medium-Grade Shale	High-Grade Shale
Fisher Assay, gpt	0	0	12	25	38
Heating Value, Btu/lb	0	800	1100	2250	3350
Moisture, %	10	2	0.24	0.25	0.3
Kerogen, %	0	0	7.17	14.46	21.75
Char, %	0.3	4	0	0	0
% Ca	14.64	13.08	12.36	11.38	10.40
% Mg	4.63	4.13	3.91	3.60	3.29
% Na	1.08	0.96	0.91	0.84	0.77
% K	2.97	2.64	2.50	2.31	2.11
% Si	17.87	15.95	15.08	13.88	12.69
Loss on Ignition, %	10.3	23	28.08	33.75	39.45

At the 110 megawatt capacity, the quantity of solid waste (fly ash plus bottom ash) using limestone as a sulfur sorbent was calculated to be 29,400, 72,850, and 17,940 lb/hr for Peabody A, Peabody B, and Salt Creek coals, respectively. If the oil shales listed in Table 1 were used instead of limestone, the calculated quantity of solid waste varied from 33,800 lb/hr for high-grade shale to 35,000 lb/hr using previously combusted shale, all with Peabody A coal. For Peabody B coal, the respective range for the different shales varied from 74,100 to 98,550 lb/hr. For Salt Creek coal, the solid waste varied from 18,500 to 18,800 lb/hr. The break-even costs for the Nucla power plant are presented in Table 2 for when oil shale begins to compete with limestone at $20.90 per ton.

Conclusions

The limestone or oil shale requirements and waste quantities generated were very strong functions of the sulfur and ash contents of the coal and the sulfur dioxide limits imposed by the regulatory agencies. The break-even point at which oil shale begins to compete economically with limestone at $20.90 per ton varied from $11.40 to $26.76 per ton.

Since the passage of the Clean Air Act of 1990, the federal requirement of an additional 70% removal of sulfur, even when burning low-sulfur coals, was removed. The economics therefore now favor the burning of low-sulfur coals to meet emission standards.

Table 2. Break-Even Oil Shale Cost When Oil Shale Competes Economically with Limestone

	Peabody A Coal	Peabody B Coal	Salt Creek Coal
Combusted Shale	$13.24	$11.90	$17.65
Retorted Shale	$14.80	$14.25	$18.21
Low-Grade Shale	$15.09	$15.64	$18.50
Medium-Grade Shale	$17.70	$20.49	$20.09
High-Grade Shale	$19.92	$26.76	$21.68

Related Publication

Nordin, J.S., and C.Y. Cha, 1989, The Use of Oil Shale as a Sulfur Sorbent in a Circulation Fluidized-Bed Combustor, Subtask 1.2 Technology Assessment, Subtask 1.3 Economic Evaluation. Laramie, WY, WRI-89-R016.

TREATMENT OF WELL-BLOCK PRESSURES IN RESERVOIR SIMULATION

Frank M. Carlson
Charles G. Mones

Background

A method of dealing with wells in grid blocks of reservoir simulators was developed by Peaceman (1978). This method continues to be very popular today (Desbarats 1993; Sharpe and Ramesh 1992). In the development for uniform grid spacing by Peaceman, a new definition of well-block pressure appeared along with a rather enigmatic constant, 0.2 (or more precisely, 0.198506 [Peaceman 1983]), which when multiplied by the grid size, gave an equivalent radius of the well block. Peaceman defined this well-block pressure as the steady-state flowing pressure at the equivalent radius.

Yet, there were others (van Poolen et al. 1968; Coats et al. 1974) who maintained that the well-block pressure should be the average pressure which should occur at a radius of 0.342 (or more precisely, 0.342198, to give it the same numbers of digits as Peaceman's constant) times the grid spacing. Because Peaceman's well-block pressure is neither the average pressure of the well block, nor is it located at the appropriate position for the average pressure, corrections are generally required to average pressure data obtained from pressure transient analysis before input to the simulator to accommodate Peaceman's method (Mattax and Dalton 1990).

Objective

The objective of this study was to more fully explore this controversy and to demonstrate that the more appropriate constant should indeed be 0.342198 when used with the procedure described below.

Procedures

Point-Centered Grids

Before focusing on the main issue of this study, a brief review of point-centering of grids is in order. A more complete review can be found in Aziz and Settari (1979). Figure 1 shows two examples of point-centered grids for both a one-dimensional system such as might be used in modeling a laboratory core flood and a two-dimensional system such as might be used in modeling a symmetry element of a pattern study (e.g., quarter of a five-spot).

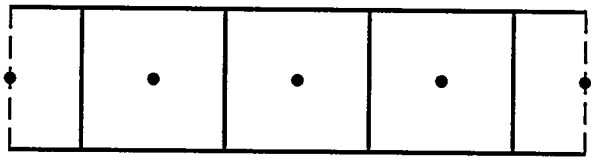

(a) One-Dimensional Point-Centered Grid

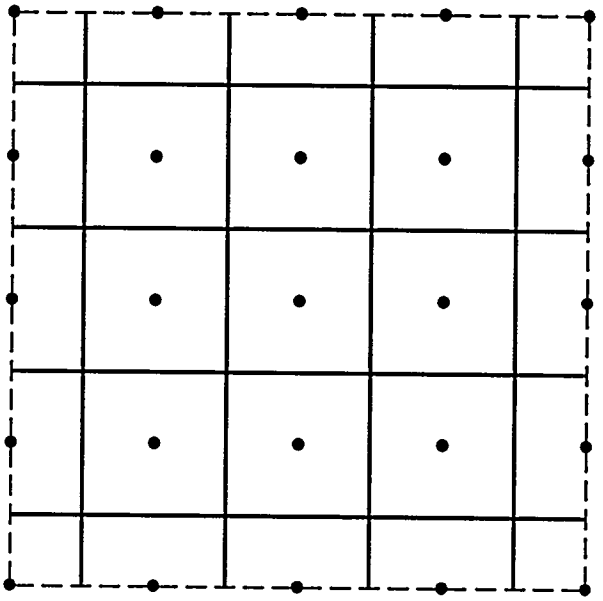

(b) Two-Dimensional Point-Centered Grid

Figure 1. Examples of Point-Centered Grids

It is for these types of systems, where the outer boundary corresponds to an injection or production face or well, that point-centered grids are most advantageous.

To construct a point-centered grid system, one specifies the distances between grid points and then draws lines midway between the grid points. These lines delineate the grid-block boundaries as shown in Figure 1. Although, this procedure can lead to grid points that are not centered within the blocks when the grid points are unequally spaced, this study concerns itself only with grid blocks which are equally spaced. Therefore, half blocks appear at the ends of the one-dimensional system shown in Figure 1(a) and on the edges of the two-dimensional system shown in Figure 1(b). Also, quarter blocks appear in the corners of the two-dimensional system.

While having the grid points on the ends, edges, and corners of such systems has the advantage of being able to locate injection or production faces or wells at the points, it also produces a distinct disadvantage. This disadvantage is that the average pressure of the half or quarter block, which should be used in the expansion terms of the finite difference equations of the reservoir simulator, does not correspond to the grid point pressure. A similar disadvantage exists when radial wells are located at grid points in the middle of square blocks, regardless of whether the grid point is on the boundary or internal to the system; but in this case, it is the nonlinearity of the radial pressure distribution that causes the problem. Dealing with these disadvantages is the major focus of this study.

One-Dimensional System

In the lower portion of Figure 2 is shown the pressure distribution for steady-state, single-phase, incompressible fluid flow for the system shown in the upper portion of the figure. Here, five equally spaced grid points have been chosen to represent a total system length L of 100 ft. In all applications that follow, the initial pressure was set to 1000 psi, the production pressure to 1000 psi, the injection pressure to 1100 psi, k to 1 Darcy, ϕ to 0.2, μ to 1.135 cP, and c to 1.0×10^{-6} psi^{-1}. The model was run until steady-state conditions prevailed. These choices are completely arbitrary and are used purely for illustration. The general form of the finite difference equation for all grid points other than grid points 1, 2, NI-1, and NI is:

$$\frac{p_{i-1}^{m} - p_{i}^{m}}{\Delta x} + \frac{p_{i+1}^{m} - p_{i}^{m}}{\Delta x} = \frac{GBV}{GP}\left(p_{i}^{n+1} - p_{i}^{n}\right) \qquad (1)$$

where, m = n or n+1 depending upon whether the equations are solved explicitly or implicitly (Mattax and Dalton 1990), GBV = grid block volume, Δx (Area), GP = group of variables, 6.328k (Area) $\Delta t/\phi\mu c$, and Area = 1 ft^2. In the models developed for this work, all equations were solved for pressure explicitly, but the same approach, to be discussed below, was later successfully implemented in an implicit model. Equation (1) defines flow between internal grid points for a slightly compressible fluid.

Before discussing the remaining equations associated with the grid system shown in Figure 2, a comment regarding the auxiliary point is appropriate. The auxiliary point is not a new grid point added to the system. Rather, it eventually turns out to be the location of the grid point pressure for the half block on the ends displaced from its original position to a point $C \cdot \Delta x$ from the end, where C is a constant between 0 and 1, but excluding 0 and 1. The original point then becomes the boundary point of injection and is only used to implement the boundary condition.

The remaining equations describing the system shown in Figure 2 are:

$$Q_{in} = \frac{6.328k\,(Area)\,(p_{inj} - p_{x1}^{m})}{\mu \cdot C \cdot \Delta x} \qquad (2)$$

$$Q_{out} = \frac{6.328k\,(Area)\,(p_{xNI}^{m} - p_{prod})}{\mu \cdot C \cdot \Delta x} \qquad (3)$$

$$\frac{p_2^m - p_{x1}^m}{(1-C)\Delta x} + \frac{Q_{in}\mu}{6.328k\,(Area)} = \frac{GBV}{2GP}\left(p_{x1}^{n+1} - p_{x1}^{n}\right) \quad (4)$$

$$\frac{p_{NI-1}^m - p_{xNI}^m}{(1-C)\Delta x} + \frac{Q_{out}\mu}{6.328k\,(Area)} = \frac{GBV}{2GP}\left(p_{xNI}^{n+1} - p_{xNI}^{n}\right) \quad (5)$$

$$\frac{p_{x1}^m - p_2^m}{(1-C)\Delta x} + \frac{p_3^m - p_2^m}{\Delta x} = \frac{GBV}{GP}\left(p_2^{n+1} - p_2^{n}\right) \quad (6)$$

$$\frac{p_{NI-2}^m - p_{NI-1}^m}{\Delta x} + \frac{p_{xNI}^m - p_{NI-1}^m}{(1-C)\Delta x} = \frac{GBV}{GP}\left(p_{NI-1}^{n+1} - p_{NI-1}^{n}\right) \quad (7)$$

By specifying C and solving the system of Equations (1) through (7) for pressure through a number of time steps until steady-state conditions prevail, the pressure distribution shown in the lower portion of Figure 2 will result, Q_{in} will equal Q_{out}, and both Q_{in} and Q_{out} will equal the steady-state flow rate,

$$Q_{ssl} = \frac{6.328k\,(Area)\,(p_{inj} - p_{prod})}{\mu L} \quad (8)$$

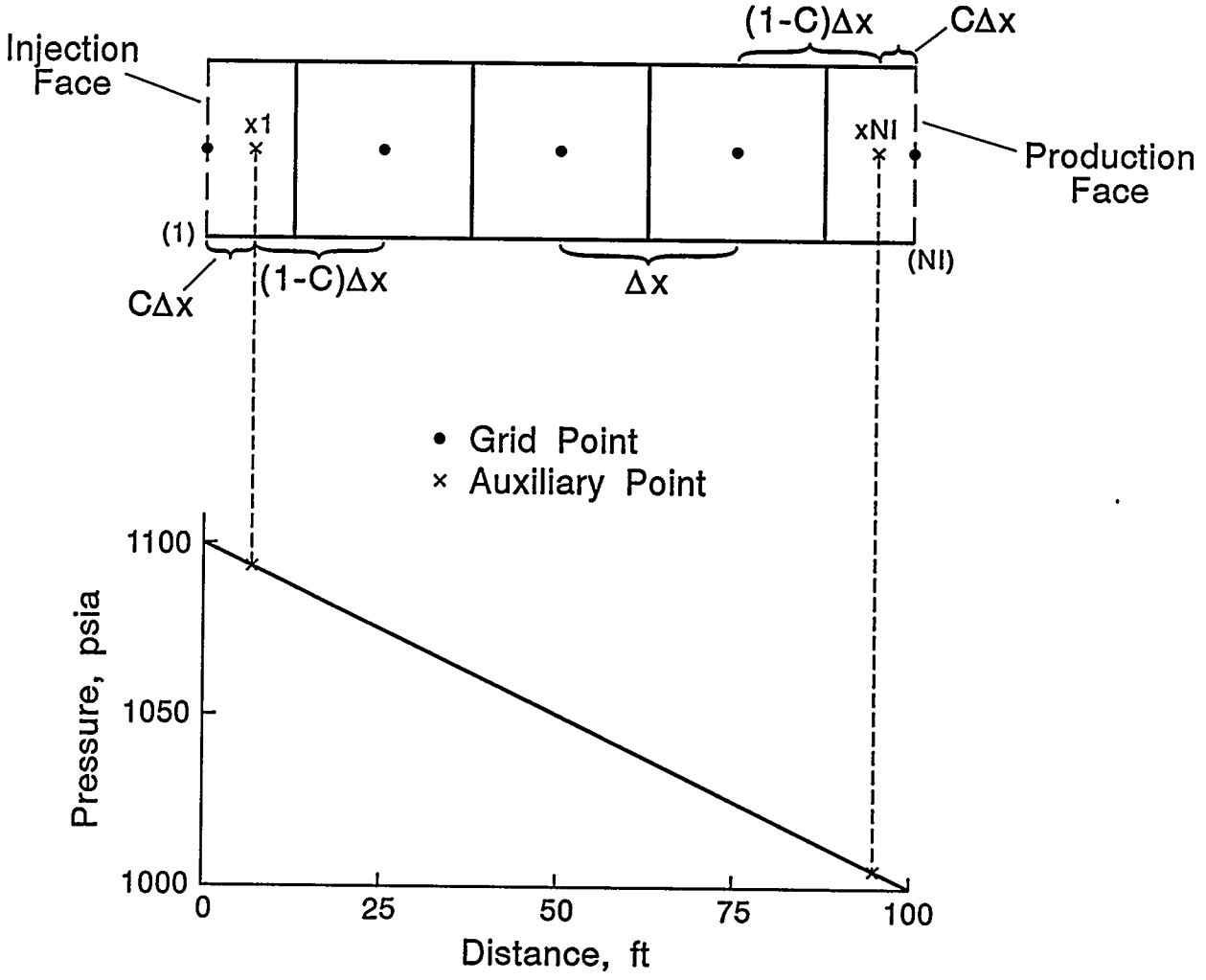

Figure 2. Developmental Point-Centered Grid and Corresponding Pressure Distribution for Linear, Steady-State Incompressible Flow of a Single-Phase Fluid

Two-Dimensional System

In the following, four sets of equations will be developed: (1) grid points other than the boundary points; (2) grid points along the left boundary excluding the injection well point, the point adjacent to the injection well, and the corner point (NI,1); (3) the corner point (NI,1); and (4) the injection well point and point adjacent to the injection well point on the left boundary. The general form of the finite difference equation for all grid points other than the boundary points for the system shown in Figure 3 is:

$$\frac{\Delta y\,(p^{m}_{i-1,j} - p^{m}_{i,j})}{\Delta x} + \frac{\Delta y\,(p^{m}_{i+1,j} - p^{m}_{i,j})}{\Delta x} + \frac{\Delta x\,(p^{m}_{i,j-1} - p^{m}_{i,j})}{\Delta y} + \frac{\Delta x\,(p^{m}_{i,j+1} - p^{m}_{i,j})}{\Delta y} = \frac{GBV}{GP}\,(p^{n+1}_{i,j} - p^{n}_{i,j}) \qquad (9)$$

where, m = n or n+1 depending upon whether the equations are solved explicitly or implicitly (Mattax and Dalton 1990), GBV = grid block volume ($h\Delta x\Delta y$), GP = group of variables ($6.328kh\Delta t/\phi\mu c$), and h = 1 ft.

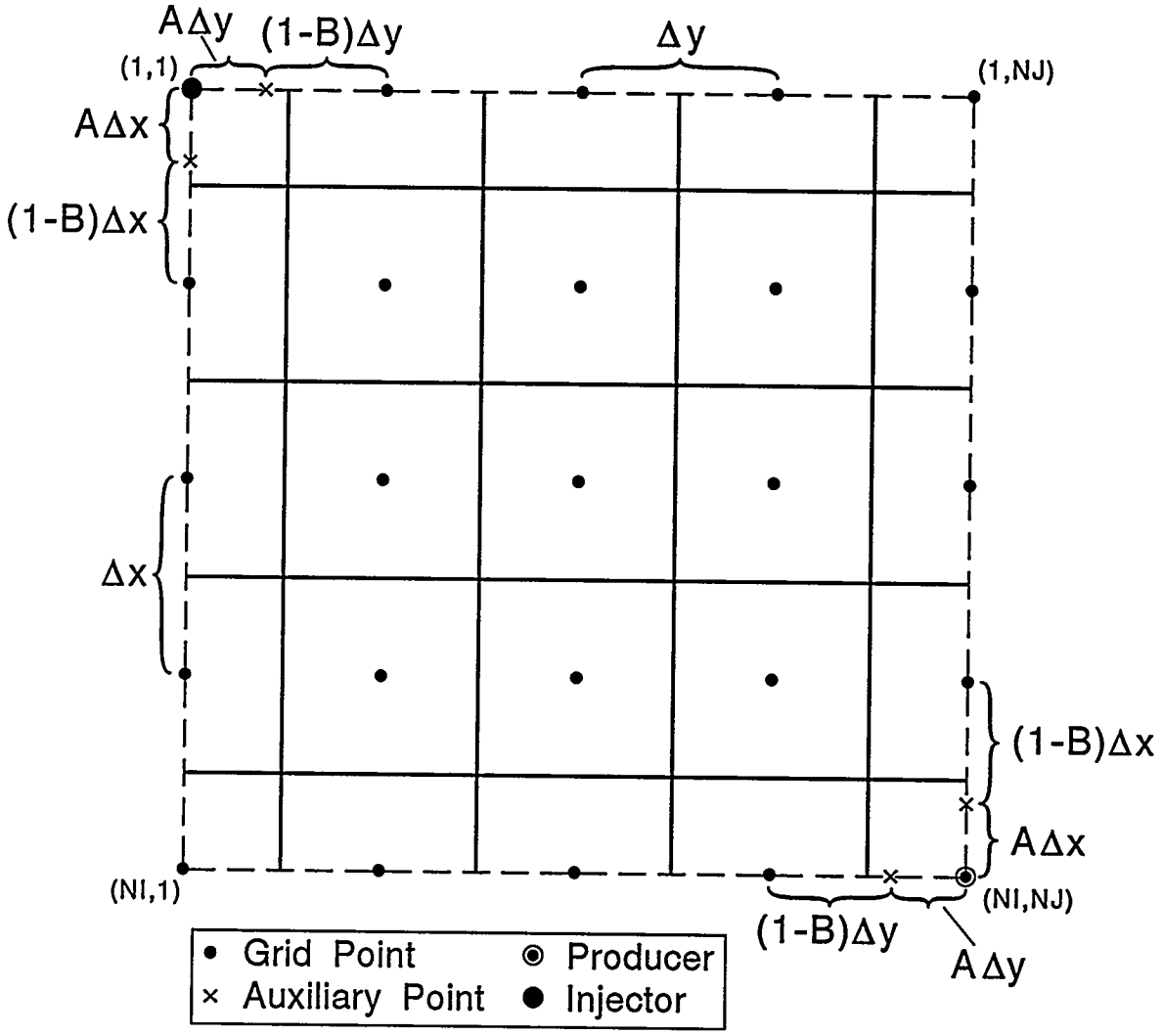

Figure 3. Developmental Point-Centered Grid for Two-Dimensional Fluid Flow in a Quarter Five-Spot Pattern

The general finite difference equation describing flow between grid points along the left boundary shown in Figure 3 for grid points other than (1,1), (2,1), and (NI,1) is:

$$\frac{\Delta y\,(p^{m}_{i-1,1} - p^{m}_{i,1})}{\Delta x} + \frac{\Delta y\,(p^{m}_{i+1,1} - p^{m}_{i,1})}{\Delta x} + \frac{\Delta x\,(p^{m}_{i,2} - p^{m}_{i,1})}{\Delta y} = \frac{GBV}{2GP}(p^{n+1}_{i,1} - p^{n}_{i,1}) \tag{10}$$

The specific finite difference equation describing flow for the grid point (NI,1) in the lower left hand corner of Figure 3 is:

$$\frac{\Delta y\,(p^{m}_{NI-1,1} - p^{m}_{NI,1})}{\Delta x} + \frac{\Delta x\,(p^{m}_{NI,2} - p^{m}_{NI,1})}{\Delta y} = \frac{GBV}{4GP}(p^{n+1}_{NI,1} - p^{n}_{NI,1}) \tag{11}$$

Analogous equations to Equation (10) were written for the other boundaries and an analogous equation to Equation (11) was written for corner point (1, NJ), but these are not shown here to conserve space.

To write the equations in the vicinity of the injection and production wells shown in Figure 3, use is again made of the auxiliary point, and development of the equations will proceed very similarly to the linear case discussed above. The auxiliary point eventually will become the grid pressure to be fixed in space wherever the numerical model will produce an injection rate at steady-state conditions equivalent to the steady-state Muskat rate (Muskat 1937) for a quarter of a five-spot pattern,

$$Q_{MUSK} = \frac{19.848kh\,(p_{inj} - p_{prod})}{4\mu\,(\ln\frac{d}{r_w} - 0.619)} \tag{12}$$

where r_w is arbitrarily given the value of 0.25 ft.

For an injection pressure of 1100 psi, a production pressure of 1000 psi, a length of one side of the system in Figure 3 of 100 ft, a permeability of 1 Darcy, and a viscosity of 1.135 cP, Q_{MUSK} = 76.445 ft^3/day.

The remaining equations needed to describe the flow along the left-hand boundary shown in Figure 3, (i.e., points xy1,1 and 2,1) are as follows:

$$r_x = A\Delta x \tag{13}$$

$$Q_{r_{inj}} = \frac{39.695kh\,(p^{m}_{inj} - p_{xy1,1})}{\mu \ln\frac{r_x}{r_w}} \tag{14}$$

$$\frac{\Delta y\,(p^{m}_{2,1} - p^{m}_{xy1,1})}{(1-B)\Delta x} + \frac{Q_{r_{inj}}\,\mu}{6.328kh} + \frac{\Delta x\,(p^{m}_{1,2} - p^{m}_{xy1,1})}{(1-B)\Delta y} = \frac{GBV}{4GP}(p^{n+1}_{xy1,1} - p^{n}_{xy1,1}) \tag{15}$$

$$\frac{\Delta y\,(p^{m}_{xy1,1} - p^{m}_{2,1})}{(1-B)\Delta x} + \frac{\Delta y\,(p^{m}_{3,1} - p^{m}_{2,1})}{\Delta x} + \frac{\Delta x\,(p^{m}_{2,2} - p^{m}_{2,1})}{\Delta y} = \frac{GBV}{2GP}(p^{n+1}_{2,1} - p^{n}_{2,1}) \tag{16}$$

It should be noted that xy1 (i.e., the auxiliary point) is the point which ultimately becomes the grid block pressure at point (1,1), as discussed above.

To complete the required system of equations for the model, equations analogous to Equations (14) and (15) were written for the producer and three more equations analogous to Equation 16 were written for the remaining points (1, 2), (NI-1, NJ), and (NI, NJ-1). These last five equations, however, are not shown to conserve space.

Results

One-Dimensional System

For the system described above and shown in Figure 2, $Q_{ssl} = 5.5753$ ft^3/day. At steady state, the choice of C is arbitrary between 0 and 1, excluding 0 and 1, but because only a half block is represented at the end points, a reasonable choice for C is 0.25 which places the grid pressure at the center of the half block (i.e., at a location equivalent to the location of the average pressure of the end blocks). In a more practical model than that described here, fluid properties would be pressure-dependent and using C = 0.25 would allow these fluid properties to change as the average pressure of the half block changes, which seems reasonable when other possible values of C are considered. Without considering the matter further in this paper, however, it is suggested that other choices for C might be more appropriate as the compressibility of the system changes (e.g., the point where the grid block pressure equals the average pressure would be different for an ideal gas than for the slightly compressible fluid described here).

Two-Dimensional System

In the resulting model, pressures were solved for explicitly (Mattax and Dalton 1990) and the solution advanced in time until steady-state conditions prevailed. At these conditions, the injection rate and the production rate of the model should be equal and both should equal Q_{MUSK} calculated from Equation 12. Importantly, however, the choice of the constants, A and B are no longer arbitrary to get the desired rate as was C in the linear case. This is because the pressure distribution at steady-state conditions is no longer linear, but is radial in the vicinity of the wells (see Figure 4 which shows the steady-state pressure distribution along the diagonal between injector and producer and was constructed from the isobars shown in Figure 236, page 577 [Muskat 1937]). The constants A and B were specified, the model run until steady-state conditions prevailed, and the resulting rates were compared with Q_{MUSK}. By trial and error the constants were changed and the model run again until the rate from the model equaled Q_{MUSK}. For the 5 x 5 grid system shown in Figure 3, the required constants turned out to be A = B = 0.3293.

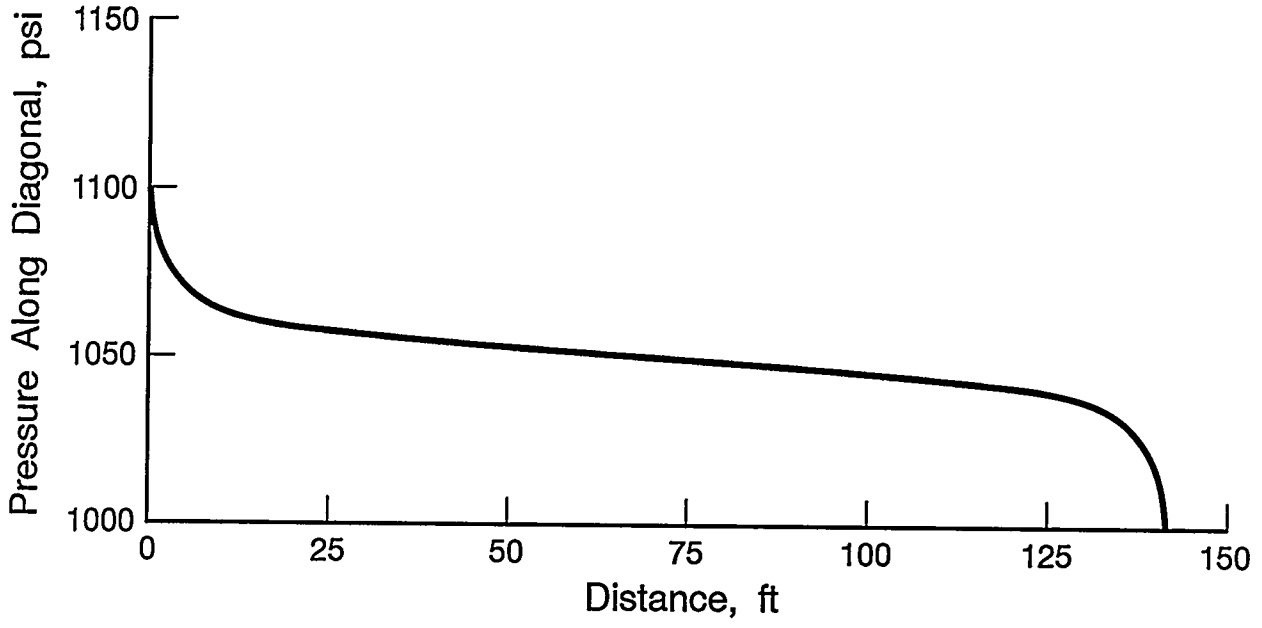

Figure 4. Steady-State Pressure Distribution along Diagonal between the Injector and Producer shown in Figure 3 for a Single-Phase Incompressible Fluid (after Muskat 1937)

For a 51 x 51 grid system, the constants turned out to be A = B = 0.3415. Even smaller grid spacings could have been tried, but at this point, the controversy mentioned in the introduction was recalled and the value of 0.342198 was placed in the model and the model run for 5 x 5, 11 x 11, 21 x 21, and 51 x 51 systems. These systems correspond to grid spacings of 20 ft, 10 ft, 5 ft and 2 ft respectively. The deviation in percent was calculated between Q_{MUSK} and the model rate at steady-state conditions. These errors are small and are plotted as the lower curve in Figure 5. Note that an extrapolation of this curve to the point where the grid spacing would be equal to r_w suggests that the error would be close to zero. Actually, such a state could never be achieved, because of the singularity in Equation 14 when $r_x=r_w$.

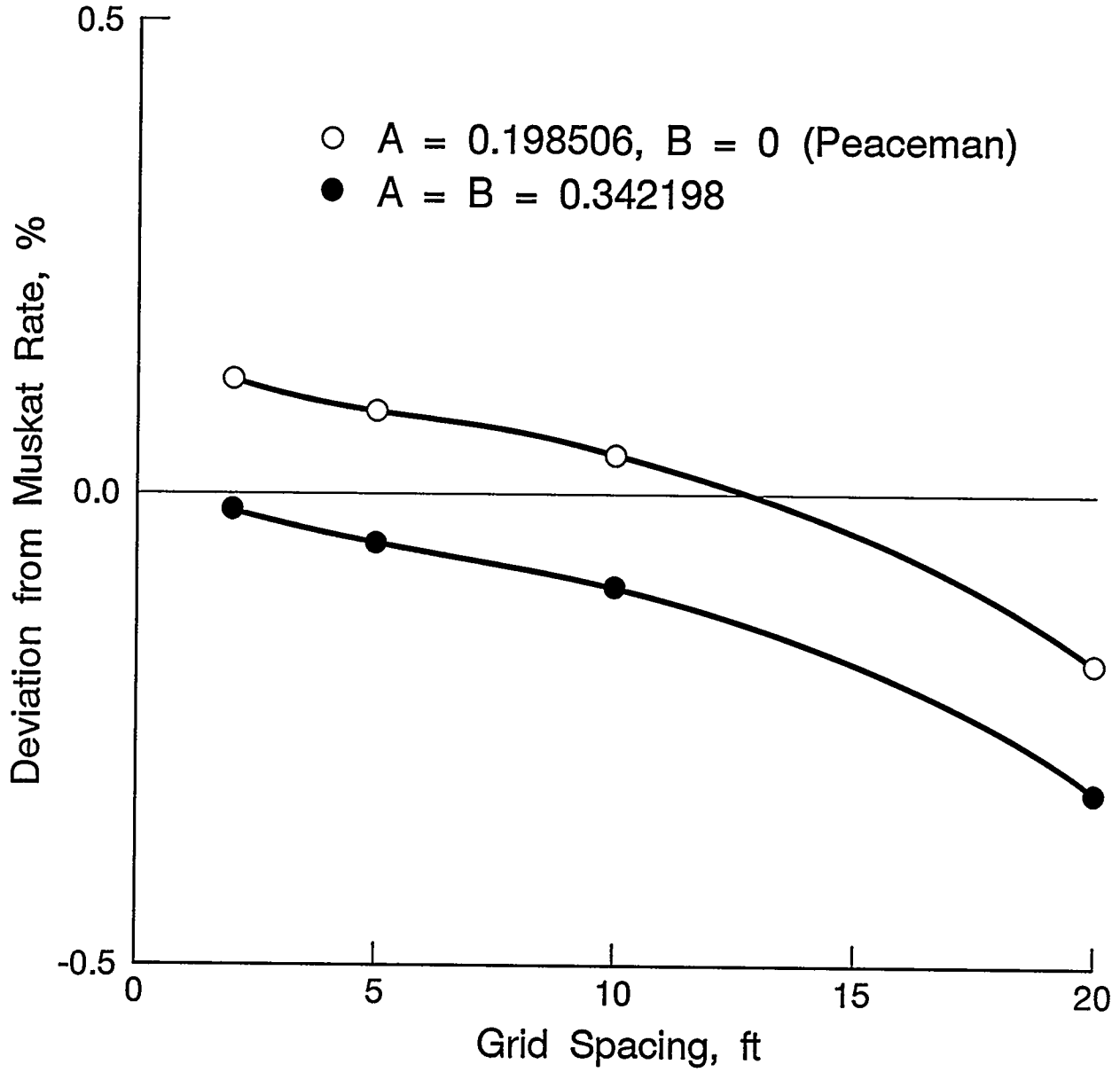

Figure 5. Errors between Numerically Predicted Steady-State Flow Rates in a Quarter Five-Spot Pattern of an Incompressible Fluid and the Flow Rate Obtained from Muskat's Equation

This may explain the slight upward trend in error when the grid spacing is 2 ft. The upper curve represents the resulting errors for the same series of model runs, but for the case where A=0.198506 and B=0. This is equivalent to Peaceman's approach (Peaceman 1978). Note that while the errors are on the same order of magnitude in both approaches, the constant of 0.198506 is empirically based while the constant of 0.342198 is analytically based. The latter constant can be derived analytically by assuming that the well-block pressure is equal to the areal average pressure (Peaceman 1978) and is the basic assumption of Van Poolen (1968) which is clearly more intuitively appealing.

Not only does the use of of the constant 0.342198 in the procedure developed here seem more appealing, but also there are several additional advantages to its use. First, as mentioned in the introduction, Peaceman's technique requires adjustments to average pressures obtained from pressure transient analysis. The technique employed here does not require such adjustments because the pressure calculated corresponds to the average pressure in the well grid block. Second, in more practical models, where fluid properties change with pressure, these properties are evaluated at the average pressure of the well block, which seems more reasonable than other possible choices. Third, for a given grid spacing, some 70% (calculated from the the ratio of 0.342198 to 0.198506) larger wellbore radii can be accommodated by the technique discussed here than by using Peaceman's technique before the singularity discussed above develops. This may be important when using the apparent wellbore radius concept when wells are extensively and vertically fractured (Earlougher 1977). Fourth, even larger wellbore radii can be accommodated using the technique outlined here by leaving the constants A = B subject to later change after model development. For example a choice of A = B = 0.9 in the 5 x 5 case above led to only a 1.9% error in the predicted rate from Q_{MUSK}. The choice of A = B = 0.9 results in a value of r_x from Equation (13) of 18 ft for the 5 x 5 system. Therefore, a value for r_w can approach this value also. The potential user of this technique is cautioned, however, that when anything other than 0.342198 is used, rigor is lost and the user does so with consequences unevaluated here. Such consequences for extremely large wellbore radii should be more thoroughly evaluated before extensive use. It does seem possible that using this technique for large wellbore radii may be no worse than assuming the fracture behaves like an effective radius to begin with, an assumption that becomes less valid with increasing fracture length.

Implementation of the Procedure in an Existing Model

At first exposure, the above technique may seem quite cumbersome to implement. While more bookkeeping is necessary, it can be fairly easily implemented in existing models. For example, it has been successfully implemented in WRI's fully implicit thermal simulator.

Because in the general case wellbores may not be fully penetrating nor a well may not continuously operate during a simulation, dynamic modification of transmissibilities in the vicinity of the well block is required. This means, for example, if a well was penetrating only three of five vertical blocks, it would be desirable to modify the transmissibilities for the active blocks but not modify the transmissibilities for the inactive blocks. For simplicity, the procedure to be described here considers only one dimension, but treatment of the other dimensions would be treated analogously. Figure 6 identifies certain spatial terms to be used in this discussion. As mentioned above, when point-centered grids are used, grid block faces are assumed to be positioned midway between the grid points. The transmissibility between points i and i+1 is, for example:

$$T_i = \frac{kA\ 6.328}{\Delta x_i} \qquad (17)$$

where, $\Delta x_i = x_{i+1} - x_i$

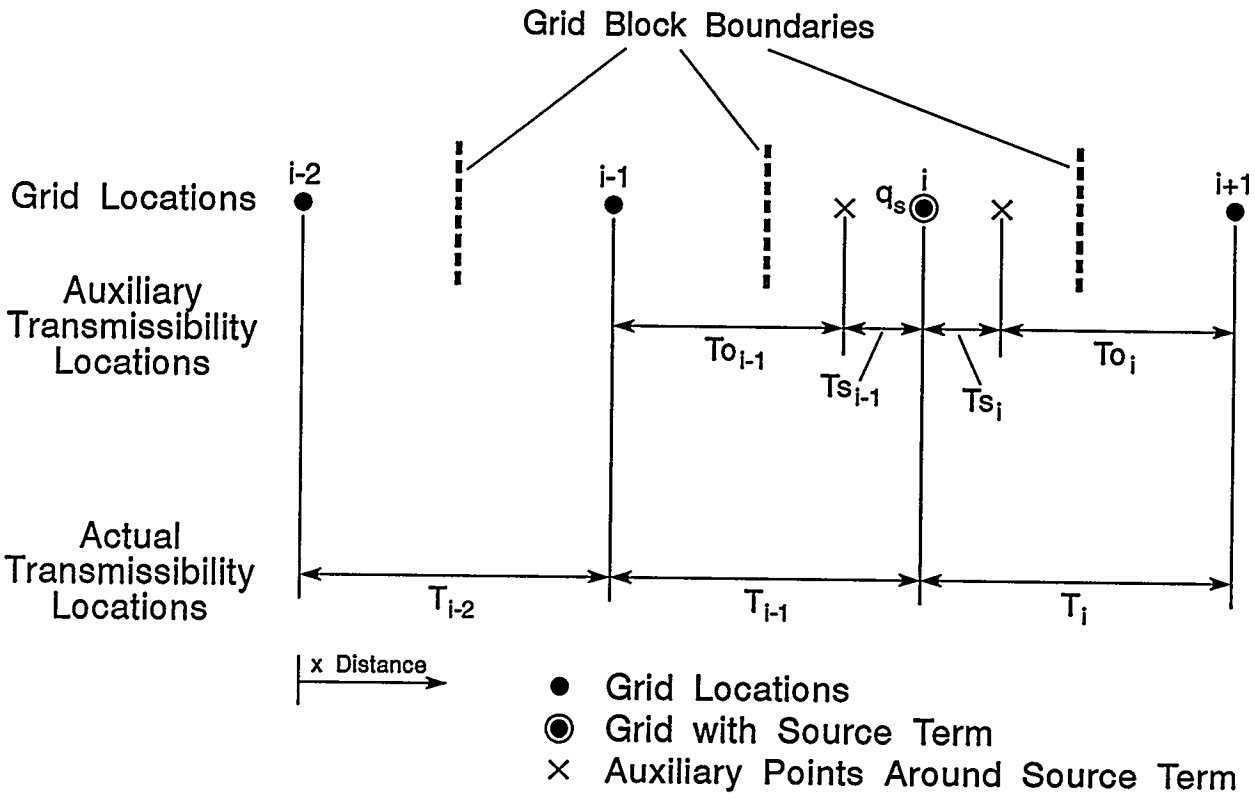

Figure 6. Representation of Transmissibilities for General Model Implementation

For a grid location containing a flowing well represented by a source term in the model, auxiliary points that locate the correct average pressure are needed to calculate the associated auxiliary transmissibility terms. For flow between adjacent grid points, two auxiliary transmissibilities are required: T_s associated with the grid point location containing the source term and T_o associated with the grid point adjacent to the grid point at which the source term is located. T_s is used to calculate interblock flow between the source point and the auxiliary point, while T_o is used to calculate interblock flow between the auxiliary point and the grid point adjacent to the grid block containing the source term.

For example, given a source term located at i, the auxiliary transmissibilities required to calculate interblock flows are as follows:

For flow between points i-1 and i,

$$T_{o_{i-1}} = \frac{6.328\,kA}{(1-\delta)(x_i - x_{i-1})} \qquad (18)$$

for interblock flow at point, i-1, and

$$T_{s_{i-1}} = \frac{6.328\,kA}{\delta(x_i - x_{i-1})} \qquad (19)$$

for interblock flow at point i.

For flow between points i and i+1,

$$T_{o_i} = \frac{6.328\,kA}{(1-\delta)(x_{i+1} - x_i)} \qquad (20)$$

for interblock flow at point, i+1, and

$$T_{s_i} = \frac{6.328\,kA}{\delta(x_{i+1} - x_i)} \qquad (21)$$

for interblock flow at point, i.

Incorporation of this technique into WRI's fully implicit thermal simulator required two one-dimensional arrays (one for T_s and one for T_o) for each spatial dimension. The auxiliary transmissibilities are formed only once, at the same point in the code where the global (original) grid transmissibilities

are calculated. When dynamic interblock flow rates are determined about each grid point, logic within the code selects the auxiliary transmissibility T_s at any grid with an active source term and T_o at adjacent points. This procedure requires minimal computational overhead and modest additional storage.

Conclusions

- A new method has been developed which allows locating the well-block pressure at the point where the average pressure is located: (a) for the linear system, a choice of 0.25 Δx seems reasonable, (b) for the radial case, the location is fixed by the system and is located at 0.342198 Δx.

- This method does not require adjusting the average pressures obtained from pressure transient analysis, as does Peaceman's approach.

- Larger wellbore radii can be accommodated using this technique than can be accommodated using Peaceman's technique for the same size grid.

- The procedure can be fairly easily implemented on existing simulators.

Nomenclature

Greek Symbols

δ = a constant multiplied by the grid spacing to determine an equivalent radius (fraction)
Δx = grid spacing in x direction (ft)
Δy = grid spacing in y direction (ft)
Δt = time step size (days)
μ = viscosity (cP)
ϕ = porosity (fraction)

Italicized Variables

A = cross-sectional area open to flow for transmissibility (ft^2)
c = compressibility (psi^{-1})

Other Variables

Area = cross-sectional area open to flow (ft^2)
A = constant multiplier of one side of a square grid block in two-dimensional system (fraction)
B = 0, for Peaceman case
A, otherwise (fraction)
C = constant multiplier of grid block size in one-dimensional system (fraction)
d = distance between injector and producer (ft)
GBV = grid block volume (ft^3)
GP = group of variables identified in text and depending upon whether system is one-dimensional (ft^4) or two-dimensional (ft^3)
h = thickness (ft)
k = permeability (darcy)
L = system length in linear case (ft)
Q = flow rate (ft^3/day)
T = transmissibility (ft^3-cP/day-psi)
x = distance (ft)

Subscripts

i = grid point number in x direction
inj = injector
j = grid point number in y direction
MUSK= steady-state, Muskat five-spot
NI = maximum grid point in x direction
NJ = maximum grid point in y direction
o = adjacent to source term
prod = producer
r = radial
s = source-term
ssl = steady-state, linear
w = well
x = equivalent radius
x1 = auxiliary grid point at injection end for one-dimensional case
xNI = auxiliary grid point at production end for one-dimensional case
xy1 = auxiliary grid point at injector in two-dimensional case

Superscripts

m = general time step identifier
n = time step identifier for which solution is known
n+1 = next time step number beyond n for which solution is unknown

Related Presentation

Carlson, F.M., and C.M. Mones, 1994, Resolution of the Inconsistency Between Peaceman's Well-Block Pressure and the Average Pressure of the Well-Block. 45th Annual Technical Meeting of the CIM, Calgary, Alberta, Canada.

THERMAL RESERVOIR MODELING

Charles G. Mones

Background

Western Research Institute had previously developed a numerical simulator (Tar Sand Reservoir Simulator [TSRS]) that describes thermal recovery processes in porous media (Vaughn 1986). The principal application of the model was to support laboratory investigations of combustion steam technologies in tar sand resources. The laboratory simulations consisted of one-dimensional tube tests in a 3-ft long reactor and two-dimensional block tests in a 3 x 3 x 2-ft sample of reservoir material.

TSRS is a highly implicit, four-phase (oil, water, gas, and coke), multicomponent, finite difference thermal simulator. The model formulation is based on a set of individual component-mass balance, energy balance, and related constraint equations that account for accumulation, vapor-liquid partitioning, chemical reaction, injection-production, heat conduction, heat loss, and the transport of mass and energy by Darcy flow. Interblock transport of mass and energy are calculated using a single-point upstream fluid mobility and enthalpy in a five-point, block-centered, finite difference scheme on fixed-sized Cartesian grids. The components described by TSRS include condensable species (oxygen and inert gas), water (liquid and vapor), oil species (light and heavy), and coke. Source-sink terms are accommodated by specification of molar-rate at a grid-block or by specification of a source-sink pressure which is used in a one-dimensional, linear flow calculation.

TSRS proved to be a useful tool for the evaluation of laboratory-scale experiments, and the formulation of its equations were satisfactory to describe thermal recovery processes (steamflooding, combustion, flooding, hot-gas pyrolysis, and hot-water flooding) in petroleum reservoir material. In fact more recently, TSRS has been used to predict field performance from CROW™ (Contained Recovery of Oil Wastes) applications. The model's nonisothermal capability and fully-implicit formulation make it a useful tool for studying CROW, as well as other thermally-related, in situ technologies currently under development.

After its initial development, TSRS had limitations. The model was not three-dimensional and its memory management algorithms were inefficient, causing long execution times for large problems. Also, specification of input data was somewhat cumbersome and lacking in flexibility. A further limitation was that TSRS did not have provisions for well terms. TSRS permitted only the specification of a constant molar rate or a constant-pressure, linear-flow term.

Objectives

The objectives of this work were to modify and extend TSRS into a thermal simulator that is usable for field-scale problems.

Procedures

In extending TSRS for use as a field-scale, reservoir simulator, the following modifications were made to the model:

- Ability to describe one-, two-, or three-spatial dimensions
- Addition of point-centered spatial grids
- Ability to specify variable grid spacings
- Ability to describe directional permeabilities
- Ability to modify interblock transmissibilities
- Addition of radial well terms (i.e., source-sink) in both horizontal and vertical orientations
- Improvements to model numerics to reduce memory storage requirements, improve accuracy, and increase computation speed

The model was modified to accommodate one-, two-, or three-spatial dimensions by using three-, five-, or seven-point, respectively, finite difference computational griding techniques. The model uses upstream weighting for the convective terms. The harmonic averaging method was used to compute interblock transmissivity terms, because it is believed that this method gives the most realistic results, particularly in cases of significant permeability contrasts. Provision for modifying transmissibility terms from the model input file was added to permit the user to more easily specify flow anomalies within the computational grid and to aid in performance of history matching procedures where it is more convenient to modify the transmissibility than block permeability. Provision for directional permeability was added to the model to more accurately describe vertical permeability contrasts which occur frequently in reservoirs.

Variable grid-spacing was implemented in the model. Variable grids permit improved accuracy with reasonable simulation times, by allowing the user to concentrate a fine-grid mesh in areas of rapidly changing reservoir properties or fluid velocities, and coarse grids in areas of relatively small changes in properties. A grid-centered method was used as described in Settari and Aziz (1972). This technique permits improved spatial discretization accuracy over cell-centered methods and has superior accuracy when performing pattern studies.

Vertical and horizontal well (source-sink) terms were added to the model. The method employed for calculation of the productivity indices in the model was developed by Peaceman (1983) for nonsquare, anisotropic reservoirs. The implementation permits wells to be oriented in the x-, y-, or z-direction and can be located anywhere within the reservoir. Well rates can be specified as either/or both rate controlled or pressure limited for any flowing phase. In the case of multilayer well completions, flow for each phase is partitioned among layers using a method of weighted, dynamic-reservoir properties rather than a more commonly used weighted mobility method. The user may also specify a gravity gradient due to liquid level within the well.

The model's transport equations and numerical discretization methods were verified by comparing model results with analytical solutions from five-spot pattern studies and one-dimensional studies that used unit mobility ratios for both injected and produced fluids. Results from these tests were acceptable, giving agreement within 1% to the analytical results.

Results

The model's ability to simulate a three-dimensional thermal problem was verified by running the model with a Society of Petroleum Engineers comparative steamflood problem (Aziz et al. 1987). The problem was to steamflood a three-dimensional, nine-spot, heavy oil reservoir. One-eighth of the pattern was to be simulated. The oil was assumed to be nonvolatile. Because TSRS does not employ a nine-point difference method, the grid was oriented differently from that shown in the problem. The grid employed nine grids aligned between the injector well and the near producer with the far producer located diagonally at the corner (from the injection well) of the nine by five grid. The results with TSRS were generally within the range of the respondents for time of steam breakthrough, production pressure, and oil recovery.

Conclusions

WRI has been successful in adapting its previously developed laboratory-scale thermal model for use as a field-scale simulator. We anticipate significant use for the model in CROW field design applications.

Related Publications

Mones, C., 1993, Modifications to WRI's Thermal Model: Development Toward a Field-Scale Simulator. Laramie, WY, WRI-93-R033.

DEVELOPMENT OF THE CROW™ PROCESS

Lyle A. Johnson, Jr.

Background

The Contained Recovery of Oily Wastes (CROW™) process removes organic contaminants from underground by adaptation of technology used for secondary and heavy oil recovery. The CROW technology has been successfully tested in the laboratory (Johnson and Guffey 1990). Presently, the process is being prepared for field demonstration in areas contaminated with wood treating wastes and byproducts of town gas production. These demonstrations will use hot-water displacement without chemical additives. The use of chemicals with the hot water to enhance displacement and solubilization of the wastes has been tested on a preliminary basis. This chemical additive testing to identify the potential of chemical addition was conducted as part of a project for the U.S. EPA SITE Program's Emerging Technology Program. The preliminary testing showed that less than 1 vol % of chemical in the initial pore volumes of hot-water flush could reduce the contaminant content by an additional 10 to 20 wt %. This testing showed the potential of chemical addition, but additional testing was needed to demonstrate the full benefit of chemical addition. The chemicals that have been tested are totally biodegradable and pose little, if any, environmental threat. However, the fate of added chemicals is considered in all testing.

The use of surfactants to enhance the solubility of polynuclear aromatic hydrocarbons (PAH) has been tested in the laboratory by researchers at Carnegie Mellon University for PAHs in water and soil-water systems (Edward et al. 1991, 1992; Liu et al. 1991; Laha and Luthy 1992). In these studies the researchers found that solubility enhancements as great as a factor of two can be attained when commercially available nonionic surfactants, such as alkyl or alkylphenol polyoxethylene, are added to the water in concentrations between 0.1 and 1.0% by volume. This solubility enhancement resulted in 70 to 90% solubilization of the PAH. Noted in these studies was the linear decrease in the surface tension between the PAH phase and the aqueous phase as the surfactant concentration increased from the onset of surfactant micelle formation (~0.1% by volume) to the critical micelle concentration (~1% by volume). The researchers also found that the partitioning of the surfactant between the soil and solution phases increased as the degree of solubility increased. The combined effects of lowering of the surface tension and the enhancement of the PAH solubility should significantly increase the removal efficiency of the CROW process.

WRI has also conducted a limited number of other CROW screening tests with chemical enhancement. The chemicals in these tests ranged from commercial surfactants to pH modifiers for the injected water. In these tests, the surfactants performed more effectively than the pH modifiers. Results of these tests are not available for public dissemination because of the proprietary nature of the work.

Objective

The objective of this study was to obtain sufficient baseline data to show the effectiveness and environmentally safe use of chemicals, primarily surfactants, to enhance the CROW process.

Procedures

Eleven one-dimensional displacement tests were originally planned. The tests investigated the effect of three chemical concentrations (0, 0.5, and 1.0 vol %) at three temperatures (ambient, the projected optimum temperature, and 22°C (40°F) below the optimum temperature).

To begin testing, a characterization sample was prepared for each contaminated material. The bulk sample was

homogenized and composite samples taken for determination of fluid saturations. The soluble organic materials collected during the saturation determinations were combined to provide a sample for initial organic characterization. The viscosity, density, and distillation range were determined for the soluble organic material. The viscosity and density determinations were conducted at ambient, 38, and 60°C (100 and 140°F) for estimation of the optimum water injection temperature.

The reactor system used for the displacement tests was a tube reactor with a disposable chlorinated polyvinyl chloride tube. The tube was vertically oriented within a series of insulated shield heaters and equipped with six internal and six external thermocouples spaced approximately every 6 inches to monitor and control the reactor and process temperatures. The entire system was interfaced to a data acquisition computer that recorded temperatures, pressures, and flow rates every 5 minutes.

Water was injected into the bottom of the reactor by a positive displacement metering pump. The injected water passed through a heater to generate steam or hot water. Chemical, when used, was metered into the water stream by a syringe pump prior to the heater.

Produced fluids were collected from the top of the reactor through an automatic sampling valve system. Sampling intervals could be held constant or changed throughout the progress of the test. The reactor back pressure was maintained at atmospheric pressure by venting the product collection vessels to the atmosphere through a gas collection system.

All experiments were conducted in the same manner, with only the temperature and chemical concentration varied between tests. To initiate the tests, a homogenized bulk sample of the contaminated sample was packed into the reactor tube. During packing of the tube, a composite sample of the material placed in the tube was collected for determination of the initial organic saturation of each tube. The weight of the packed material was recorded. The tube was instrumented with the appropriate thermocouples and placed into the reactor shell.

Following placement of the tube, water injection at 100 cc/min and the predetermined temperature was initiated and continued until 40 pore volumes (PV) of water had been injected. The PV of the packed tube was determined from the physical dimensions of the tube and the density and saturation of the contaminated soil. During the displacement phase, produced fluids were sampled every 2 to 4 PV for total organic carbon (TOC) determinations, and measurement of the pH and resistivity. At the end of each test, a 2-liter sample of the produced fluid was collected, labeled, and placed in cold storage until completion of the project. The purpose of these samples was to provide material for assisting in the determination of the surfactant partitioning if the post-test materials were not sufficient.

After completion of the injection phase, the injection and production ports were closed, the reactor shell opened, and the tube allowed to cool before removal. The cooled tube was then removed from the reactor shell and the weight of the contents determined and recorded. The flushed material was then extruded from the tube and divided into five even increments from the top to the bottom of the tube. Each increment was homogenized and a composite sample analyzed to determine the post-test organic saturation distribution and to track the surfactant partitioning during the test.

The planned tests were to consist of 11 one-dimensional displacement tests using a single contaminated sample. However, results of the first 11 tests indicated that a second sample would assist in interpretation of the results. The initial 11 tests were conducted in three sets of experiments, three tests without chemical addition, six tests with chemical addition, and two duplicates. In each set of tests,

three temperatures were used for the flushing water. These temperatures were based on the viscosity and density of the organic contaminate as determined during initial characterization.

Tests with the second contaminated material consisted of four tests. A single test was conducted at ambient temperature and the predicted optimum temperature with and without chemical addition. The chemical addition was at the highest concentration used in the first 11 tests.

The chemicals selected for use were Triton X-100 and Igepal CA-720, marketed by Aldrich Chemicals, and Hyonic NP-90, produced by Henkel Corporation. All three chemicals are nonionic, aerobically biodegradable surfactants. To evaluate which chemical to use, a sample of the known amount of the initial contaminated material was placed in a 1% by volume mixture and agitated for several hours. The resultant surfactant and organic mixture was decanted and the organic reduction determined. Based on these simple tests, Igepal was chosen as the chemical to be used in subsequent flushing tests. The chemical concentrations chosen for use in the flushing tests were 0.5 and 1.0% by volume. These concentrations and the initial three selected chemicals were based on the studies at Carnegie Mellon University.

The contaminated soils used in the tests were obtained from a former manufactured gas plant (MGP) site and a inactive wood treatment site. The MGP site material, the initial material, was a sandy soil contaminated with coal tars and coal cinders that was provided by Midwest Gas of Iowa. The soil from the wood treatment site was a sand contaminated with creosote and petroleum based hydrocarbons. This material was from the Baxter Tie Plant Site in Laramie, Wyoming that was provided by Union Pacific Railroad.

During the packing of the tube with the MGP soil, it was noted that the packed weights were significantly lower than with prior tested materials. The material, instead of being a sand matrix contaminated with coke and coal tars, was determined to be mainly coke-like material with some sand. The individual coke particles were porous and the contaminant appeared to reside within the particle. Therefore, the packed tubes provided a dual porosity system consisting of primary porosity between the coke and sand particles, and secondary porosity within the individual coke particle. It was decided that testing of the material would increase the knowledge of the CROW process, so testing was continued.

Results

The initial nine tests, 128 through 136, with the MGP soil consisted of one each at approximate flushing temperatures of 18, 57, and 79°C (65, 135, and 175°F) with 0, 0.5, and 1.0% by volume chemical added to the flushing water (see Table 1). For all tests, the targeted injection rate was 100 cc/min and a total injected volume of ~40 PV. Results of the initial nine tests indicate a slight increase in the reduction of the organic contaminant with increasing flushing temperature, but no definite effect from the chemical addition (the solid symbols in Figure 1). The slight increase in organic removal is believed to be caused by the location of the contamination in the secondary porosity, where only a minor contact with the flushing water occurs. However, the TOC analyses of the produced fluids and determinations of the chemical remaining in the residual organics (organics remaining on or in the matrix following flushing) indicated that a portion of the chemical was partitioning into the contaminant.

To assist in determining the effect of the chemical addition, tests 137 and 138 were conducted at the two higher temperatures with 1.0% chemical addition, replication of the conditions in tests 132 and 135, respectively. The difference between these tests was the incorporation of an additional ~40 PV of elevated temperature flushing following the initial ~40 PV of elevated temperature flushing with chemical addition.

Table 1. Test Parameters and Results

Test No.	Init. Oil Sat., Dry	Porosity, %	Temp., °F	% Chemical Added	Inj. Rate cc/min	Inj. Water PV	Residual Sat., Dry	Organic Red., %
Midwest Samples								
128	10.27	41.74	67	0.00	109.00	33.3	8.90	13.34
129	11.11	33.62	135	0.00	89.00	44.1	9.01	18.90
130	12.55	44.71	175	0.00	93.00	33.0	9.67	22.95
133	11.77	43.84	63	0.46	107.00	33.0	9.78	16.91
136	9.85	46.51	134	0.50	92.00	31.3	8.16	17.16
134	11.75	45.61	174	0.49	102.00	35.4	9.58	18.47
131	10.62	38.04	65	0.80	99.00	38.7	10.01	5.74
132	12.14	41.99	139	0.90	96.00	36.5	9.27	23.64
135	12.23	46.03	178	0.92	100.00	34.1	9.79	19.95
137	11.78	39.75	141	1.00	98.00	76.3	7.55	35.91
138	11.00	45.04	173	0.93	99.00	64.0	6.00	45.45
Baxter Samples								
139	1.97	27.15	67	0.00	86.00	47.6	1.10	44.16
140	1.25	25.35	64	0.95	101.00	47.2	0.52	58.40
141	1.16	29.98	149	1.09	87.00	41.3	0.35	69.83
142	1.97	33.93	152	0.00	98.00	36.9	1.07	45.69

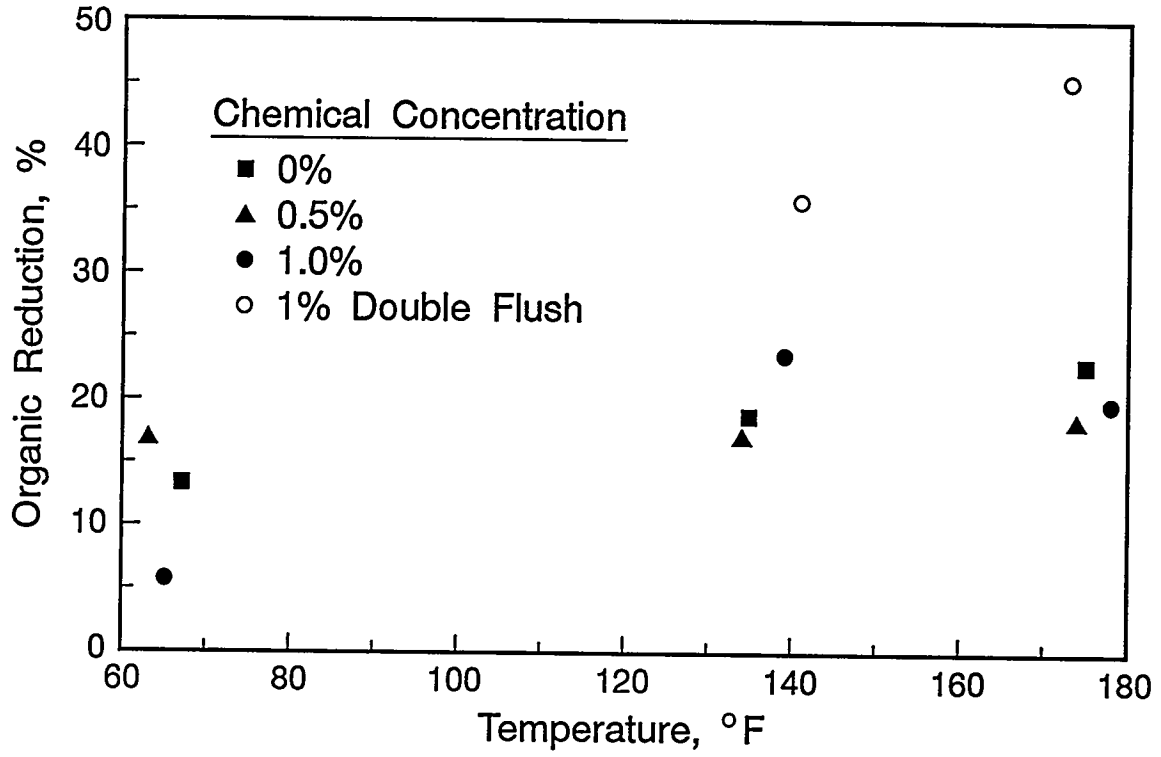

Figure 1. Organic Reduction versus Flush Temperature, Midwest Tests

As shown in Figure 1, the additional 40 PV of flushing produced a significant increase in the organic reduction. This indicates that the chemical additive is modifying the solubility and the surface tension of the contaminate such that the organic material can be removed from the secondary structure, but the process requires extended flushing following the initial chemical-added flushing.

Because the results using the MGP soil were inconclusive, it was decided that a contaminated soil with a matrix that was essentially sand might help determine the effect of chemical addition. The soil from the Baxter Tie Plant was selected. Only four tests, 139 to 141, were conducted using this material. The tests were conducted at ambient temperature and 66°C (150°F) at chemical concentrations of 0 and 1.0% by volume. These tests showed that increased flushing temperature resulted in a slight increase in organic removal, while the addition of chemical resulted in a significant increase in organic removal at all temperatures tested (Figure 2). Also noted was a significant increase in organic removal with chemical addition at the elevated temperature.

Conclusions

Results of the laboratory tests of the CROW process using chemical assisted flushing on two contaminated materials indicate:

- Elevated flushing temperatures increase the removal of the organic contaminate compared to ambient temperature flushing. This is true for both the no-chemical and chemical flushing series.
- The addition of chemical results in increased removal of the contaminate at all temperatures tested for material with primarily a sand matrix.
- Chemical added to the flushing water of a material consisting of secondary porosity systems will increase the recovery, but will require additional nonchemical flushing of the system to allow time for solubilization and surface tension modification effects to occur.
- The chemical partitioned between the aqueous and soil phases occurred with a significant concentration remaining in the residual organic. This is especially evident when the soil is comprised of porous particles.

Related Publication

Johnson, L.A., Jr., 1994, Development of the CROW™ Process. Laramie, WY, WRI-94-R017.

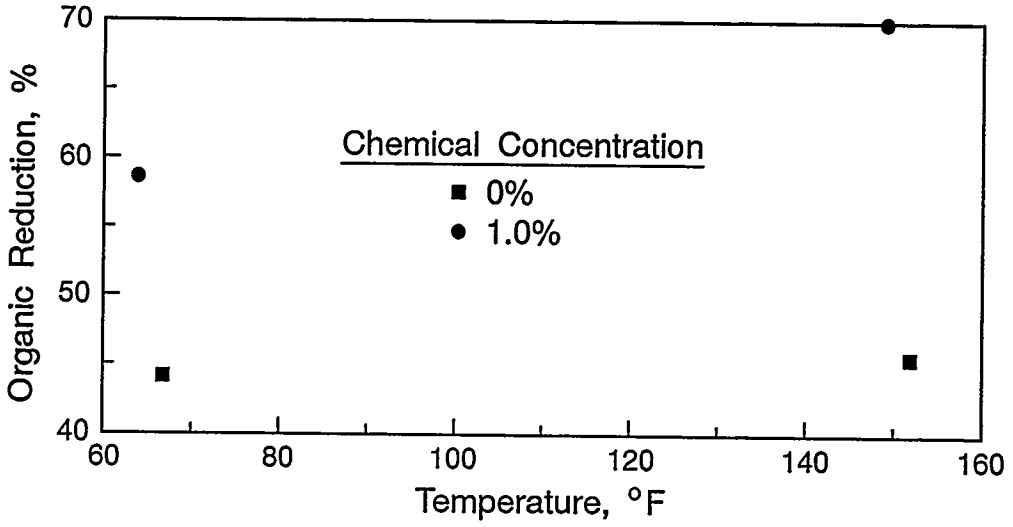

Figure 2. Organic Reduction versus Flush Temperature, Baxter Tests

STEAMFLOOD ENHANCEMENT IN NATURALLY FRACTURED RESERVOIRS

Robert M. Satchwell
Lyle A. Johnson, Jr.

Background

Steamflooding is the primary enhanced oil recovery process in use today, both in project number and the oil produced (Moritis 1992). However, steamflooding of naturally fractured reservoirs is currently not viable, resulting in a virtually untapped resource. Chemically enhanced steamflooding could unlock these reserves. The literature reveals several attempts to produce fractured reservoirs by conventional steamflooding with limited success (Sahuquet and Ferrier 1982; Britton et al. 1983; Dietrich 1986; Oballa et al. 1991). The DOE steamflood field tests in the Northwest Asphalt Ridge tar sand deposit (Johnson and Thomas 1985) and in the Shannon formation at National Petroleum Reserve No. 3 (NPR-3) have been influenced by heterogeneous reservoir conditions. Primary recovery from the NPR-3 Shannon formation has been projected to be less than 6% of the original oil in place, with only an additional 9% from steamflooding because of the fractured nature of the Shannon formation (U.S. Department of Energy 1988).

Improvements to the performance of the steamflood process with chemical additives can provide application to a wider range of reservoirs, including those that are naturally fractured. Laboratory investigators have shown that selected classes of new cross-linked polymers have the potential for use in the harsh steamflood environment (Sydansk 1988; Mumallah and Doe 1989; Jones and Shu 1990). These polymers have had limited field testing, but with encouraging results (Cooke and Eson 1992; Hunter et al. 1992). Foaming agents for such service have a similar status, having been developed in the laboratory (Navratil et al. 1983), but having had only limited field testing (Mohammadi et al. 1991). In the present study, a series of laboratory experiments was conducted to evaluate various chemical enhancements. These included incorporation of surfactants, polymers, and noncondensible gases into the steamflood process.

Objectives

The objectives of this study were to identify and test potential additives that would modify flow in fractures and divert it to the porous media during steam injection. Specific tasks were to: (1) identify potential additives from a literature review, (2) test and evaluate these potential additives in one-dimensional (1-D) experiments and identify the best additive, and (3) perform three-dimensional (3-D) experiments with the best additive of the 1-D tests to verify its performance and effectiveness in modifying flow in fractures.

Procedures

The 1-D simulations were performed using fluid saturated 2-inch diameter by 12-inch long Berea sandstone cores in a rubber sleeved core holder. In all tests, a steam injection rate of 18.04 cc/hr cold water equivalent was obtained with a positive displacement pump feeding a heater. Steam flowed through a bypass system until the desired steam quality conditions were established, at which time the steam was directed into the core. In all tests, steam was injected until a residual oil saturation was achieved. Chemical injection into the sample was then initiated, as directed by the manufacturer's recommendations. During each test, the produced fluid was collected on a scheduled basis. The oil-water ratio was determined either by direct measurement or by centrifugation, if necessary. Following the tests, the core was removed from the test cell, and the water and residual oil saturations were determined by extraction.

Twenty-five 1-D tests were performed at temperatures ranging from 93 to 228°C (200 to 443°F) and outlet pressures between 1 to 217 psig, using 10 separate Berea sandstone cores with and without simulated fractures. Fractures were simulated by placing spacers between the core-halves.

Two 3-D simulations were conducted using 24 x 24 x 18-inch blocks of actual Shannon reservoir material. In both experiments, an injector and producer were located diagonally across from each other within each sample block. In both cases, an injection pressure of 250 psig was maintained during the steaming, with thermocouples monitoring the movement of the front. After the produced water cut exceeded 95%, the selected additive was injected. The first test simulated a horizontal fracture that intersected both production and injection wells. To create this fracture orientation, the large block was cut into two smaller 24 x 24 x 9-inch blocks and placed back together. The second test simulated a vertical fracture case. This fracture orientation was created by cutting the large block into two smaller 12 x 24 x 18-inch blocks. In both cases, 0.006-inch spacers were placed between each of the smaller blocks to maintain fracture width.

Results

A literature review was conducted and potential sources were contacted to gather relevant information for additives to be evaluated in 1-D simulations. The selection of the additives was dictated by high-temperature stability. The additives selected for testing were three polymers and a surfactant. The additives were: Chevron's Chaser SD 1020 (surfactant), EPT's cross-linked EPT-HY- TEMP polymer gel (Polymer 1), Pfizer's cross-linked FLOPERM 3429-340X4 (Polymer 2), and Coalplex's HCC 1000 Polymer (Polymer 3).

Results of the 1-D tests indicated that the surfactant obtained the largest additional oil recovery after steamflooding to residual oil saturation, (see Table 1). Recovery was lower when the spacer width was increased from 0.000 to 0.006-inch with all additives, except with Polymer 1. However, the increase in recovery with Polymer 1 at higher spacer widths was statistically insignificant. Core-to-core variance was determined to be insignificant, since several tests were performed using the same core, but with different additives.

Table 1. Percentage Reduction in Oil Saturation with Respect to Spacer Width

Spacer Width	Additive Type			
	Surfactant	Polymer 1	Polymer 2	Polymer 3
Whole	1.54	na	na	0.54
0.000-inch	3.37	0.27	2.49	2.35
0.006-inch	0.56	0.47	0.71	0.80
Average of Fracture Cases	1.96	0.37	1.60	1.57

The injection of all additives caused the injection pressure to increase. However, with all polymers, the high-temperature steam removed the blockage, and subsequent injection pressure decreased.

Since the surfactant produced the best results in the 1-D simulations, 3-D simulations were performed using the surfactant. The production for the horizontal fracture case is presented in Figure 1. The figure shows the cumulative production of oil and water. Also illustrated in Figure 1 is the projected oil production for the steamflood, exclusively. Approximately 16.3% more oil was produced by the addition of the surfactant. The cumulative water production was offset, but the slope was nearly identical in the stabilized portion of the test.

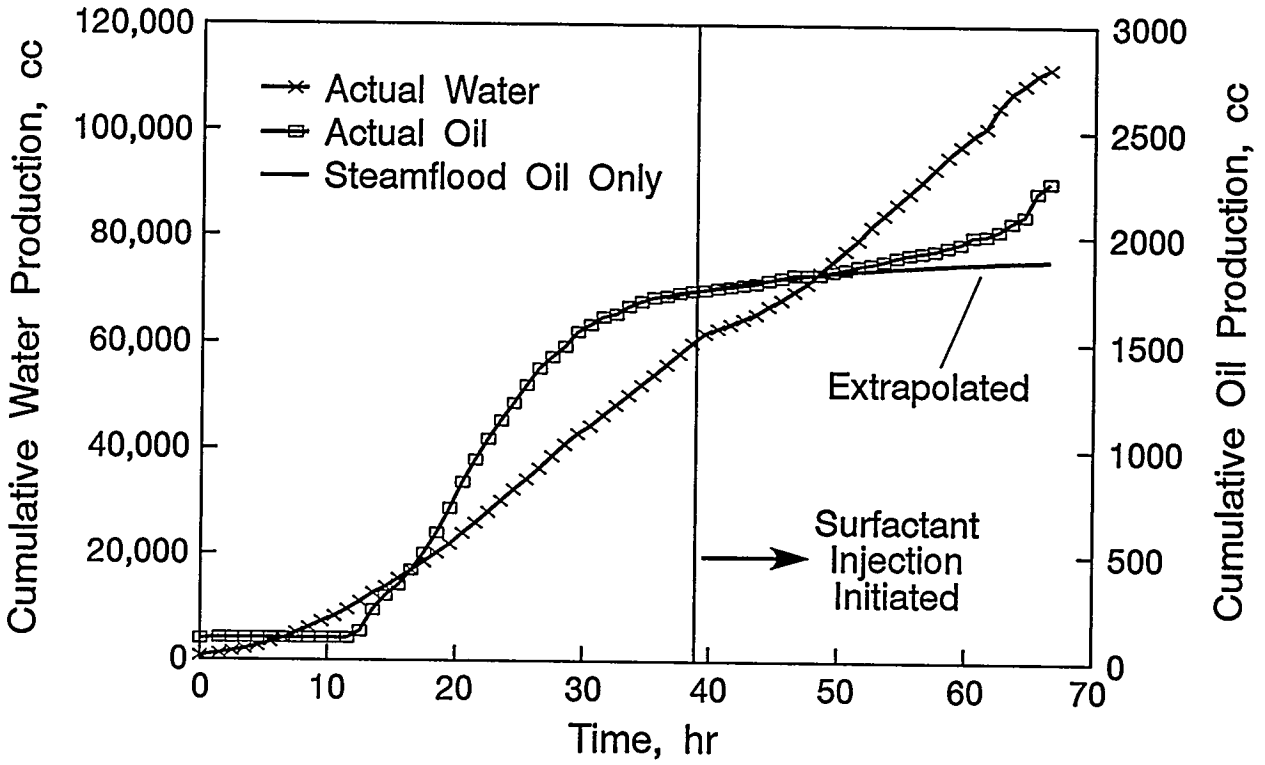

Figure 1. Cumulative Production for Horizontal Fracture Case

A plot of injection pressure as a function of time is shown in Figure 2. From the data it is clear that the pressure did not increase after the surfactant was injected. Based on discussions with the manufacturer of the surfactant, it was deduced that the lack of increased pressure was caused by the high quality of steam used during the test. Lack of sufficient volume of water did not create enough stable foam to divert the flow away from the fracture.

The vertical fracture 3-D test was performed under similar conditions, except nitrogen was injected to elevate the superficial velocity of the steam. The nitrogen also reduced the partial pressure of steam, which created a more stable foam. The injection rates were tailored to the wellbore dimensions to create sufficient superficial velocity to produce turbulent flow in the injection well.

The cumulative oil and water production for the vertical fracture case is shown in Figure 3. Also included is the projected oil production for the steamflood without the addition of surfactant. These results show that 31% more oil was produced by the addition of surfactant. Increased injection pressure was observed as shown in Figure 4. It was presumed that this increase was caused by stable foam under these test conditions. It should be noted that the increase in pressure persisted even when the injection rate was reduced from 35 cc/min to 10 cc/min. The injection pressure data are consistent with the manufacturer's claim that stable foam diverts the flow away from the fracture.

Conclusions

This study identified and tested four potential additives to modify flow in fractures and divert it to the porous media during steam injection. Several 1-D and 3-D laboratory tests were performed on fracture media.

The 1-D laboratory tests showed that a surfactant additive was more effective than the three polymers tested. The ineffective behavior of the polymers is believed to be caused by temperature degradation.

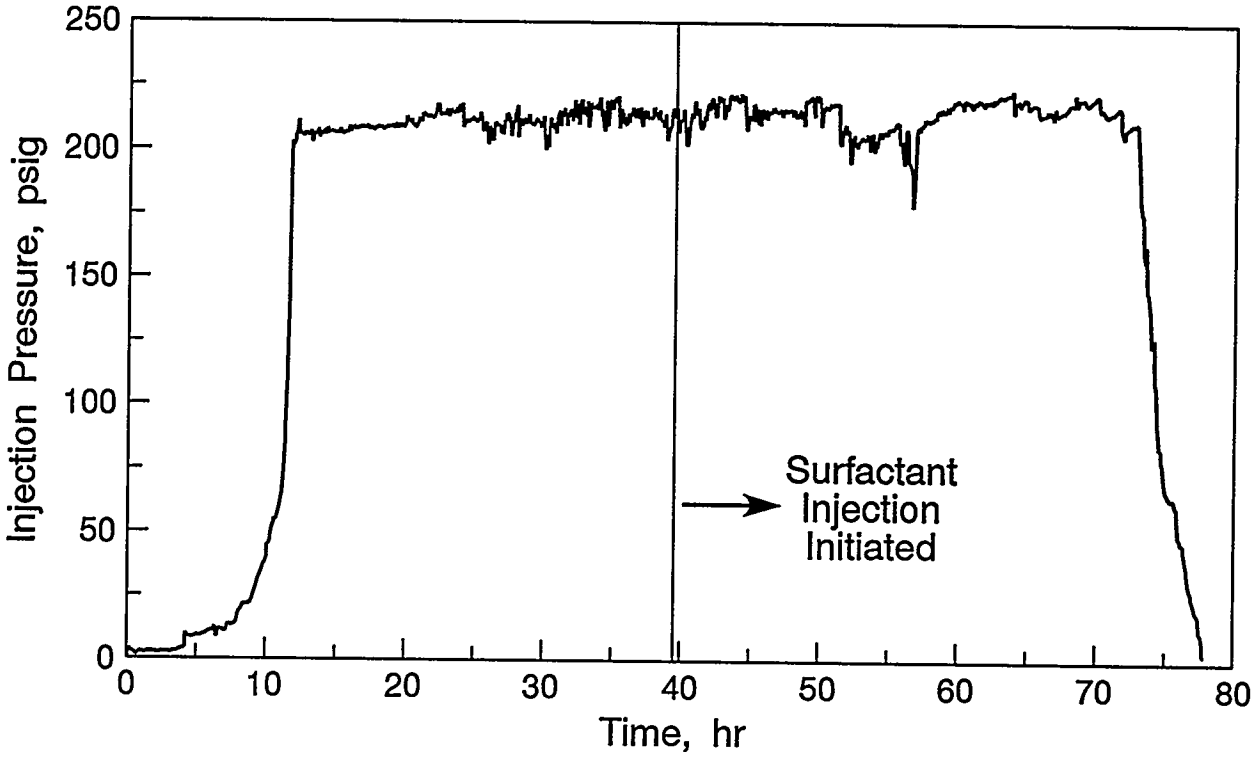

Figure 2. Injection Pressure for Horizontal Fracture Case

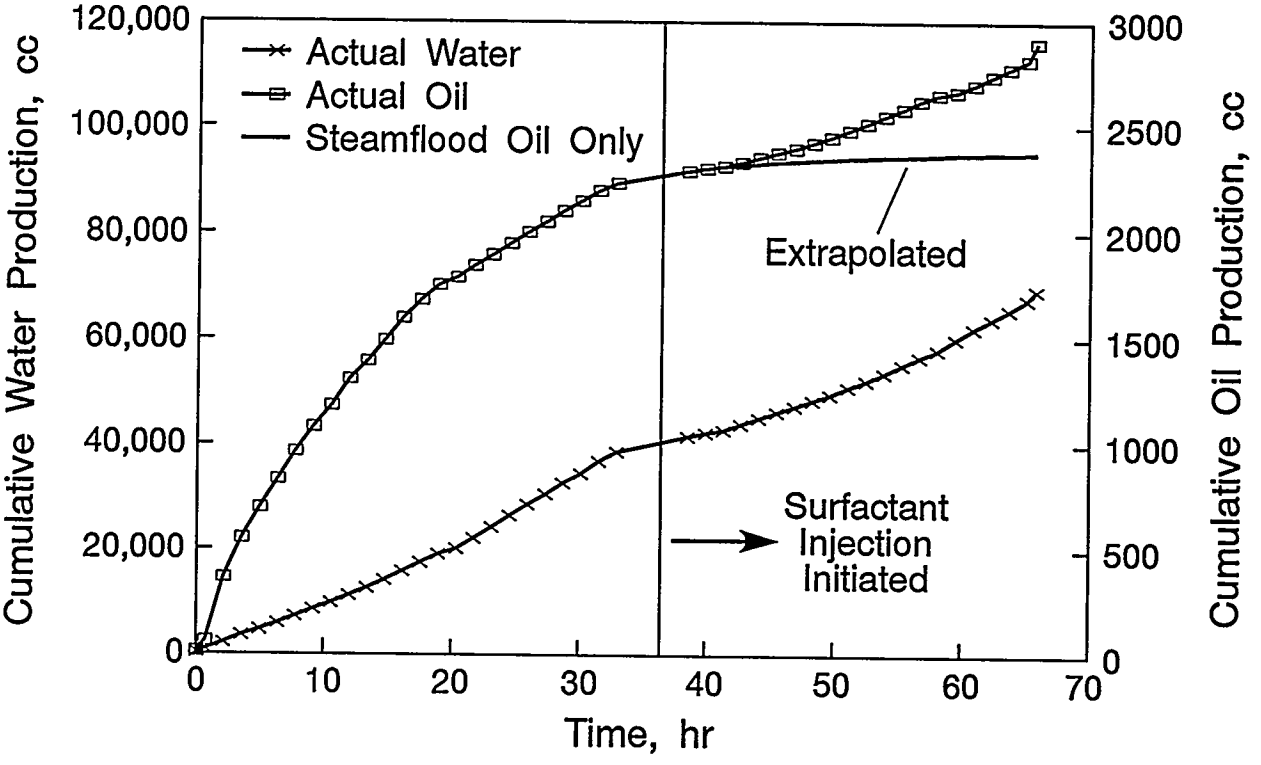

Figure 3. Cumulative Production for Vertical Fracture Case

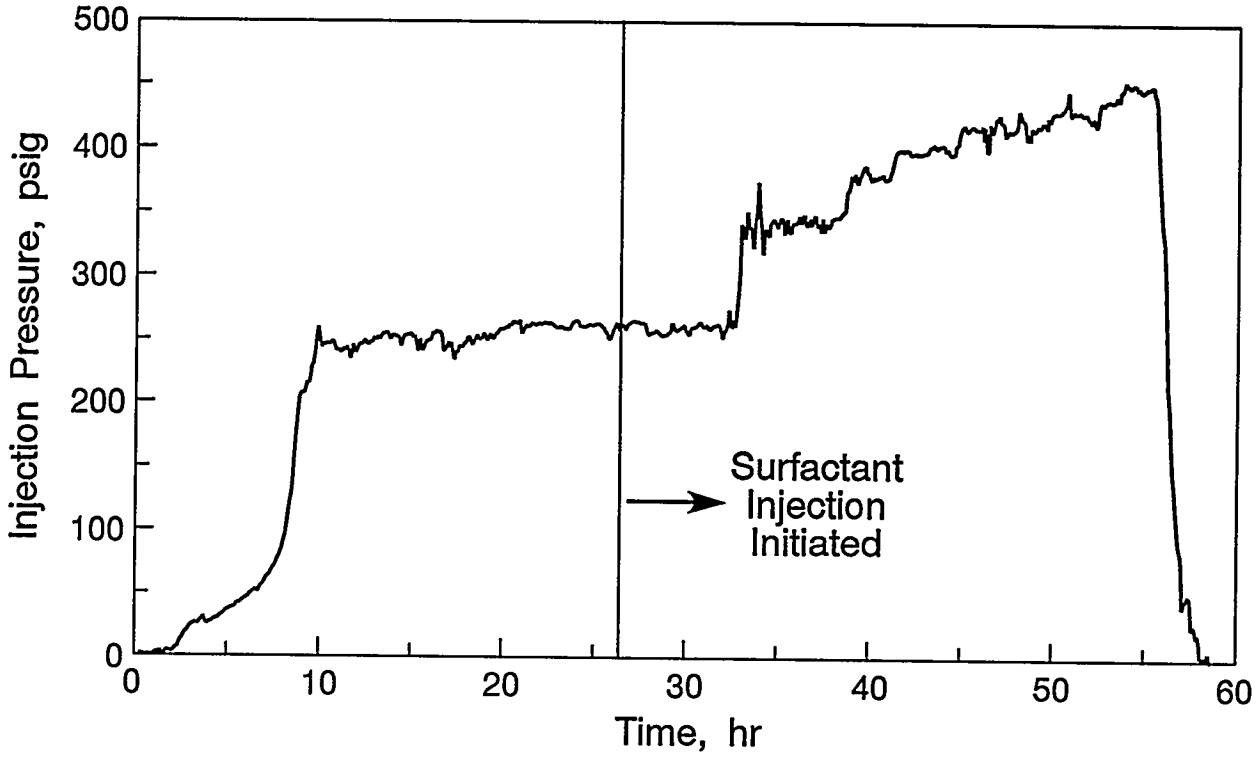

Figure 4. Injection Pressure for Vertical Fracture Case

The surfactant additive was further tested in the 3-D simulations that indicated that the preferential flow path can indeed be blocked if a stable foam is created. Off-spec tests showed that even if a stable foam was not created, improved recovery can still be obtained. Increased recovery in this case is likely created by a reduction in interfacial tension between the oil and water. However, when stable foam is created, further improvement in recovery is obtained.

The results indicate that critical parameters for use of the surfactant as a foaming agent are: (1) sufficient superficial velocity of the steam, and (2) adequate water volume in the steam to create the foam.

Further testing at a pilot demonstration level is recommended in a fractured field such as the Shannon Formation at NPR-3.

Related Publication

Satchwell, R.M., and L.A. Johnson, Jr., 1994, Steamflood Enhancement in Naturally Fractured Reservoirs. Laramie, WY, WRI-94-R018.

PRELIMINARY EVALUATION OF A CONCEPT USING MICROWAVE ENERGY TO IMPROVE AN ADSORPTION-BASED, NATURAL GAS CLEAN-UP PROCESS

R. William Grimes

Background

Increased use of natural gas can enhance U.S. energy security, environmental quality, and economic strength by decreasing our reliance on imported oil. Though natural gas has many advantages as a fuel, demand has decreased since the early 1970s (U.S. Department of Energy 1992). Technologies that enlarge and stabilize the domestic natural gas reserve base will help increase the long-term availability of affordable natural gas. Technologies that clean up low quality natural gas can also increase this reserve base and do so without increased drilling activity.

Among the contaminants common in natural gas, nitrogen is one of the more difficult to remove economically. For larger gas fields cryogenic processing can be used successfully. However, due to the high capital and operating costs of cryogenic systems, their application is restricted to larger fields, typically where production exceeds 20 MMscf/day (Minteco PSA 1991).

The widespread commercial acceptance of pressure swing adsorption (PSA) for low-volume gas separations would seem to make it a natural choice for a noncryogenic method of separating nitrogen from natural gas. The application of PSA to nitrogen-methane separation has been studied extensively, and pressure/vacuum swing adsorption cycles for bulk separation of nitrogen-methane mixtures have been developed. However, the high capital and operating costs associated with vacuum regeneration of the adsorbent limits the application of the pressure/vacuum swing process. Adsorbent regeneration also has a strong influence on the efficiency of separation processes based upon cyclic adsorption. Regeneration is a major factor controlling the amount of adsorbent needed to produce a given amount of product, and thus, the size and cost of the separation system. In fact, adsorbent regeneration tends to be the major factor in the overall economics of these processes (Lukchis 1973).

Earlier, unpublished results of work conducted at Western Research Institute involving microwave regeneration of adsorbent chars suggested the possibility that microwave energy could be used instead of vacuum pumping to regenerate adsorbents. Despite relatively high cost, microwave energy has found industrial acceptance in applications where its unique properties offer advantages that offset its cost. Direct energy transfer and homogeneous and selective heating are among the properties of microwave energy that can provide a technical advantage to compensate for the high capital cost of the equipment (Orfeuil 1987).

Williams Technologies, Inc. (WTI) has been investigating the development an economically viable wellhead PSA system to separate nitrogen contamination from natural gas. They have determined that existing PSA cycles using vacuum-assisted adsorbent regeneration are unacceptable for small gas fields. WTI investigated the performance of a variety of solid adsorbents for use in a PSA process, including various natural and synthetic zeolites and an active carbon. While they did not find a workable adsorbent, they developed process guidelines and generated data related to the performance of various solid adsorbents for the separation of nitrogen-methane mixtures. Among the zeolites tested, WTI found that the natural zeolite, chabazite, showed a strong selectivity toward methane adsorption. However, it was considered unacceptable because the adsorbed methane did not desorb on pressure reduction (Minteco PSA 1991).

Objectives

The objectives of this work were to determine if microwave energy could be used to regenerate a zeolite adsorbent and to evaluate the feasibility of using microwave energy to improve the desorption phase of a PSA process applied to the upgrading of natural gas contaminated with nitrogen.

Procedures

Because chabazite holds methane strongly, it was chosen as the adsorbent to evaluate the concept of microwave-assisted desorption. If microwave energy could increase the desorption efficiency of methane without heating of the adsorbent, it should also work with other zeolites, such as faujasite and zeolite-L, on which methane is held less tightly.

Based on the cost of nonproductive energy consumption, the criteria for evaluating the heating of the adsorbent during regeneration was set at less than 11°C (20°F) rise in adsorbent temperature due to microwave heating.

Adsorbent regeneration consists of the desorption of gas with the subsequent return of adsorptive capacity. Thus, to evaluate the concept of using microwave energy for adsorbent regeneration, an ability to measure quantities of gas adsorbed and desorbed was needed. This was accomplished using a specially designed PSA apparatus. For this evaluation, adsorption and desorption of gas was measured volumetrically. Effluent gas quantity was measured volumetrically by displacing water from six individually-selectable cylinders. The closed end of each cylinder was fitted with a rubber septum from which a sample of gas could be withdrawn for analysis. The effluent gas composition was determined using a gas chromatograph. Chabazite from the Chula Claims in Arizona was supplied by WTI for use in the tests. For each test series, approximately 100 grams of preconditioned chabazite was weighed and poured into the adsorption column.

The performance of the preconditioned chabazite was established using six adsorption-desorption pressure cycles. This also resulted in the production of saturated chabazite for the subsequent microwave desorption tests. The simple two-step pressure cycle consisted of feeding 30% N_2/70% CH_4 at a constant rate of 1183.2 scm^3/min into the column until the column pressure reached 50 psig, stopping the feed, and allowing the column to depressurize from the feed end. For each cycle, all effluent gas was collected, and its volume and composition was determined and recorded. The feed time was recorded and multiplied by the feed rate to give the volume of gas fed in each cycle.

After six pressure swing cycles, the chabazite was removed from the adsorption column and placed in a 500 mL round bottom flask. The flask was connected by a length of plastic tubing to a gas collection cylinder and placed in a microwave oven. The gas collection cylinder was located outside the microwave oven. The oven was turned on for 0, 1, 2, or 3 minutes, and the effluent gas was collected, and its volume measured. The flask was removed from the oven, and the temperature in the center of the chabazite was measured with a thermocouple probe. The regenerated chabazite from the microwave oven was then reloaded into the adsorption column, and additional pressure swing cycles were run. Effluent volume and composition of the gas streams were determined and recorded and subsequently compared to the baseline values obtained for the preconditioned chabazite.

Results

Table 1 lists the volume of methane and nitrogen in the feed and effluent from consecutive pressure swing adsorption cycles using preconditioned chabazite and chabazite regenerated for 1 and 2 minutes in the microwave oven. The effluent volume of the gases from the pressurization and depressurization portions of each cycle are listed separately. Figure 1 shows the volume of methane and nitrogen adsorbed per gram of adsorbent.

Table 1. Feed and Effluent Volumes for Selected Cycles, scm^3

Cycle	Feed		Effluent			
			Pressurize		Depressurize	
	CH_4	N_2	CH_4	N_2	CH_4	N_2
Baseline 1	2518.9	1087.3	18.7	919.5	1390.0	501.8
Baseline 2	2064.7	891.2	475.1	597.1	1399.3	479.7
Baseline 3	2050.9	885.3	537.9	462.7	1347.2	521.1
Baseline 4	2064.7	891.2	680.6	395.8	1351.3	523.9
Baseline 5	2050.9	885.3	666.8	402.7	1352.8	537.6
Baseline 6	2064.7	891.2	684.0	402.7	1327.1	522.1
One Minute 1	1584.1	683.8	11.0	52.8	1090.0	539.6
One Minute 2	1418.8	612.4	4.5	57.4	1260.5	609.6
Two Minutes 1	2424.3	1046.5	39.6	697.7	1318.5	476.6
Two Minutes 2	2024.9	874.0	455.1	480.5	1335.0	502.5
Two Minutes 3	1928.5	832.4	588.7	357.0	1340.7	500.4

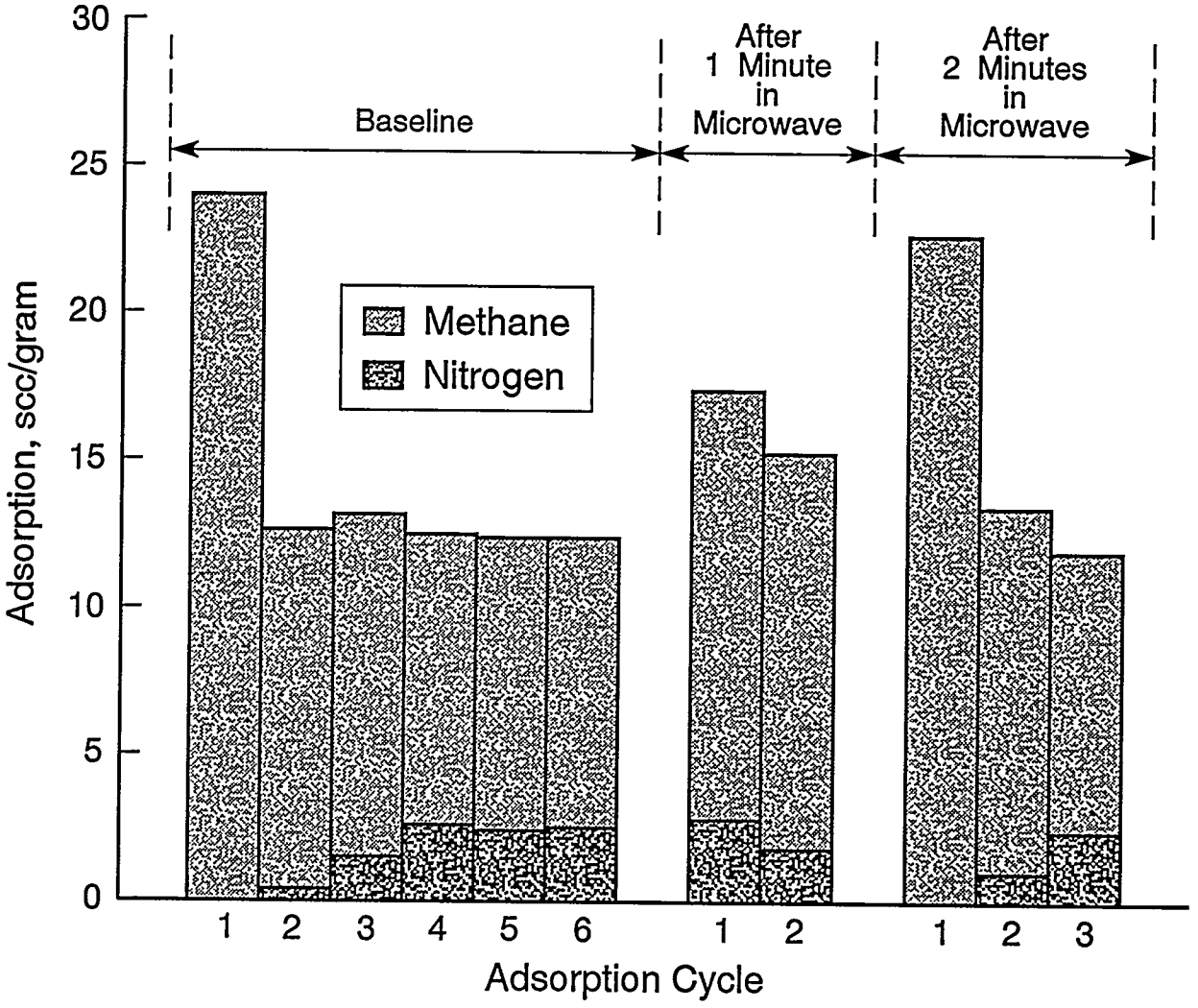

Figure 1. Methane and Nitrogen Adsorption for Selected Cycles

In the pressurization portion of the first cycle (Baseline 1), the preconditioned chabazite adsorbed 24 scm^3 of methane per gram of adsorbent (see Figure 1). Nitrogen (adsorbed from the air while the column was being loaded with adsorbent) was replaced by methane for a negative net adsorption of nitrogen in the first cycle. Very little methane was found in the waste gas stream during the pressurization portion of the cycle (2.0%), and based upon the volume and composition of this waste stream effluent from the first cycle, it can be concluded that methane was selectively adsorbed on chabazite. The depressurization effluent from the first cycle does not show significant methane enrichment (73.5 versus 70.0%). This is probably due to the fact that the column void volume and volume in the connecting tubing are filled with nitrogen at the end of the first pressurization cycle. The rapid blow-down step used in more complex cycles (Yang 1987) would increase product purity, as would desorption of more of the residual methane held by the chabazite.

Effluent from the pressurized portion of the second cycle (Baseline 2) contains a considerable amount of methane (44.3%). Methane adsorption in the second cycle is reduced to about 12.5 scm^3 per gram of adsorbent, one-half of the amount found for the first cycle. Effluent from the depressurization portion of the second cycle is very similar to that of the first cycle, with no significant methane enrichment of the product detected (74.5 versus 70.0%).

By the end of the third cycle (Baseline 3), the chabazite shows essentially no selective adsorption of methane from the gas mixture, and the composition of the effluent gas during pressurization and depressurization are nearly equal for each of the remaining three pressure swing cycles. Thus, the preconditioned chabazite shows a strong selectivity toward methane adsorption, and a methane capacity of 24 scm^3 per gram of adsorbent for the first pressure swing cycle. However, selective adsorption and capacity for methane decline rapidly, and after three cycles, there is essentially no selective adsorption of methane, and capacity is down to 10 scm^3 per gram of adsorbent.

The volume of gas desorbed and the corresponding temperature rise of the chabazite after 0, 1, 2, and 3 minutes in the microwave oven were measured. Heating of the adsorbent was evident for all three microwave exposure times. Two minutes in the microwave oven were needed to regenerate the adsorbent to the activity observed for the preconditioned adsorbent. However, this exposure resulted in a 42°C (75°F) rise in adsorbent temperature, which is considerably greater than the evaluation limit of 11°C (20°F). The methane content of the products resulting from the depressurization portion of the three cycles (Two Minutes 1, 2, and 3) averaged about 73% versus 70% in feed, an enrichment comparable to that observed for the preconditioned chabazite.

Conclusions

Microwave energy can be used successfully to regenerate a zeolite adsorbent, but excessive heating of the zeolite makes the concept impractical for application in natural gas cleanup. Microwave-assisted desorption may prove useful in adsorptive purification processes where recovery of the sorbate with minimal dilution is required.

Related Publication

Grimes, R.W., 1992, Preliminary Evaluation of a Concept Using Microwave Energy to Improve an Adsorption-Based, Natural Gas Clean-Up Process. Laramie, WY, WRI-93-R003.

ADVANCED EXPLORATORY PROCESS TECHNOLOGY REFERENCES

Aziz, K., and A. Settari, 1979, Petroleum Reservoir Simulation. Elsevier Science Publishers, London and New York.

Aziz, K., A. Ramesh, and P.T. Woo, 1987, Fourth SPE Comparative Solution Project: Comparison of Steam Injection Simulators. J. Pet. Tech., December 1987, 1576-1584.

Britton, M.W., W.L. Martin, R.J. Leibrecht, and R.A. Harmon, 1983, The Street Ranch Pilot Test of Fracture-Assisted Steamflood Technology. J. Petr. Tech., 35:3 511-522.

Cha, C.Y. and L.J. Fahy, 1989, The Use of Oil Shale as a Sulfur Sorbent in a Circulating Fluidized-Bed Combustor. Laramie, WY, WRI-89-R014.

Coats, K.H., W.D. George, and B.E. Marcum, 1974, Three-Dimensional Simulation of Steamflooding. Soc. Pet. Eng. J., December 1974, 573-592.

Cooke, R.W., and R.L. Eson, 1992, The Development of a Low-Cost Thermally Stable Polymer/Surfactant System for Steam-Sweep Efficiency Improvement. Western Regional Meeting of SPE Proceedings, Bakersfield, CA, 83-93.

Desbarats, A.J., 1993, Geostatistical Analysis of Interwell Transmissivity in Heterogeneous Aquifers. Water Resources Research, 29(4): 1239-1246.

Dietrich, J.K., 1986, Cyclic Steaming of Tar Sands Through Hydraulically Induced Fractures. SPE Res. Eng., 1:(3) 217-229.

Earlougher, R.C. Jr., 1977, Advances in Well Test Analysis. Monograph Vol. 5, Soc. Pet. Eng. of AIME, p. 154.

Edward, D.A, Z. Liu, and R.G. Luthy, 1991, Surfactant Enhanced Solubility of Hydrophobic Organic Compounds in Water and in Soil-Water Systems. In Baker, R.A., ed., Organic Substances and Sediments in Water, Lewis Publishers, 2: 383-405.

Edward, D.A, Z. Liu, and R.G. Luthy, 1992, Interactions Between Nonionic Surfactant Monomers, Hydrophobic Organic Compounds and Soil. Water Science and Technology, 26(1-2): 147-158.

Friedman, M.A., R.H. Melvin, and D.L. Dove, 1989, The First One and One-Half Years of Operation at CUEA Electric Association's 110-MW Circulating Fluidized Bed Boiler. 10th International Conference on FBC, ASME, New York, NY.

Hunter, B.L., R.S. Buell, and T.A. Abate, 1992, Application of a Polymer Gel System To Control Steam Breakthrough and Channeling. Western Regional Meeting of SPE Proceedings, Bakersfield, CA, 71-81.

Johnson, L.A. Jr., and K.P. Thomas, 1985, Comparison of Laboratory and Field Steamfloods in Tar Sand. Laramie, WY, DOE/FE/60177-1940.

Johnson, L.A., Jr., and F.D. Guffey, 1990, Contained Recovery of Oily Wastes (CROW) - Final Report. United States Environmental Protection Agency Assistance Agreement CR-815333, RREL, Cincinnati, OH.

Jones, L.G., and W.R. Shu, 1990, Temperature Activated Polymer for Profile Control. U.S. Patent 4,947,933, August 14.

Laha, S., and R.G. Luthy, 1992, Effects of Nonionic Surfactants on the Solubilization and Mineralization of Phenanthrene in Soil-Water Systems. Biotechnology and Bioengineering, 40:1-14.

Liu, Z., S. Laha, and R.G. Luthy, 1991, Surfactant Solubilization of Polycyclic Aromatic Hydrocarbon Compounds in Soil-Water Suspensions. Water Science and Technology, 23: 475-485.

Lukchis, G.M., 1973, Adsorption Systems Part III: Adsorbent Regeneration. Chemical Engineering, August 6, 1973, 86.

Mattax, C.C.,and H.L. Dalton, 1990, Reservoir Simulation. Monograph Vol. 13, Soc. Pet. Eng. of AIME.

Minteco PSA, 1991, Laboratory Results Summary for the Period June 1990 - January 1991. Unpublished report.

Mohammadi, S.S., D.A. Coombe, and V.M. Stevenson, 1991, Test of Steam-Foam Process for Mobility Control in S. Casper Creek Reservoir. Petr. Soc. of CIM and AOSTRA Preprint 91-77.

Moritis, G., 1992, EOR Increases 24% Worldwide; Claims 10% of U.S. Production. Oil and Gas J., 90:16 51-79.

Mumallah, N.A., and P.H. Doe, 1989, Gelable Compositions and Use Thereof in Steam Treatment of Wells. U.S. Patent 4,799,548, January 24.

Muskat, M., 1937, Flow of Homogeneous Fluids Through Porous Media. McGraw-Hill.

Navratil, M., M. Sovak, and M.S. Mitchell, 1983, Formation Blocking Agents: Applicability in Water- and Steamflooding. 58th Annual Technical Conference and Exhibition of SPE Proceedings, San Francisco, CA, SPE 12006.

Nordin, J., D. Cameron, and D. Sheesley, 1989, Clean Coal Technology Program; Solid Waste Management. Laramie, WY, DOE/MC/11076-2862.

Nordin, J.S., and C.Y. Cha, 1989, The Use of Oil Shale as a Sulfur Sorbent in a Circulation Fluidized-Bed Combustor, Subtask 1.2 Technology Assessment, Subtask 1.3 Economic Evaluation. Laramie, WY, WRI-89-R016.

Oballa, V., D.A. Coombe, and W.L. Buchanan, 1991, Factors Affecting the Thermal Response of Naturally Fractured Reservoirs. CIM/AOSTRA 1991 Technical Conference Proceedings, Baniff, Alberta, Can., 53-1 to 53-15.

Orfeuil, M., 1987, Electric Process Heating. Battelle Press, Columbus, OH, 558-565.

Peaceman, D.W., 1978, Interpretation of Well-Block Pressures in Numerical Reservoir Simulation. Soc. Pet. Eng. J., June 1978, 183-194.

Peaceman, D.W., 1983, Interpretation of Well-Block Pressures in Numerical Reservoir Simulation with Nonsquare Grid Blocks and Anisotropic Permeability. Soc. Pet. Eng. J., June 1983, 531-543.

Peaceman, D.W., 1993, Interpretation of Well-Block Pressures in Numerical Reservoir Simulation with Nonsquare Grid Blocks and Anisotropic Permeability. Soc. Pet. Eng. J., June 1983, 531-543.

Sahuquet, B.C., and J.J. Ferrier, 1982, Steam-Drive Pilot in a Fractured Carbonated Reservoir: Lacq Superieur Field. J. Petr. Tech., 34:4 873-880.

Settari, A., and K. Aziz, 1972, Use of Irregular Grid in Reservoir Simulation. Soc. Pet. Eng. J., April 1972, 103-114.

Sharpe, H.N., and B.A. Ramesh, 1992 Development and Validation of a Modified Well Model Equation for Nonuniform Grids with Application to Horizontal Well and Coning Problems. Reservoir Engineering, 1992 SPE Annual Technical Conference and Exhibition, Washington, DC, October 4-7, 1992, SPE #24896, 397-411.

Sydansk, R.D., 1988, A New Conformance-Improvement-Treatment Chromium(III) Gel Technology. SPE/DOE Enhanced Oil Recovery Symposium Proceedings, Tulsa, OK, 99-114.

Synfuels Engineering and Development, 1988, Oil Shale as a Sulfur Sorbent in a Circulating Fluidized Bed Combustor. Report to Electric Power Research Institute, Palo Alto, CA.

U.S. Department of Energy, 1988, Reserve Estimates Naval Petroleum Reserve No. 3. Unpublished Report.

U.S. Department of Energy, 1992, Natural Gas Strategic Plan and Multi-Year Crosscut Plan, FY 1993-1998. DOE/FE-0251P.

van Poolen, H.K., E.A. Breitenbach, and D.H. Thurnau, 1968, Treatment of Individual Wells and Grids in Reservoir Modeling. Soc. Pet. Eng. J., December 1968, 341-346.

Vaughn, P., 1986, A Numerical Model for Thermal Recovery Processes in Tar Sand: Description and Application. Laramie, WY, DOE/MC/60177-2219.

Yang, R.T., 1987, Gas Separation by Adsorption Processes. Butterworth Publishers, Stoneham, MA.

ADVANCED FUELS RESEARCH

EVALUATION OF WESTERN SHALE OIL AS A FEEDSTOCK FOR HIGH-DENSITY AVIATION TURBINE FUEL

Kenneth P. Thomas

Background

The processing of alternate fossil fuels has been the subject of several studies sponsored by the U.S. Department of Energy and the U.S. Department of Defense. For the most part, these studies evaluated conventional petroleum processes for the production of specification-grade fuels. For example, Sullivan et al. (1978) and Sullivan and Frumkin (1986) studied conventional refining processes for the production of transportation fuels from shale oils and coal-derived liquids. Moore et al. (1981) studied the production of military jet fuels from western shale oil by a process that combined hydrogenation, acid extraction of nitrogen compounds, and fluid catalytic cracking. A combination of hydrogenation, acid extraction, and hydrocracking was also studied by Reif et al. (1982) for converting western shale oil to jet fuels. Other research sponsored by the U.S. Air Force investigated the conversion of tar sand oils and heavy petroleums to military jet fuels (Moore et al. 1987; Talbot et al. 1986). These studies demonstrated that conventional aircraft turbine fuels could be made from several unconventional fossil fuel sources.

Objective

The purpose of this investigation was to determine the feasibility of producing high-density aviation turbine fuel from western shale oil.

Procedures

The processes that were evaluated included acid-base extraction, solvent dewaxing, Attapulgus clay treatment, coking, and hydrogenation. Acid-base extraction was used to reduce the heteroatom content of middle distillates and atmospheric and vacuum gas oils. Solvent dewaxing was used to reduce the paraffin content of atmospheric and vacuum gas oils. Attapulgus clay treatment was used to reduce the heteroatom content of middle distillates. Coking was used to reduce the molecular weight and distillation range of vacuum gas oils. Hydrogenation was used to reduce the heteroatom content and to saturate the aromatic rings of middle distillates and atmospheric gas oils.

A whole shale oil sample received from the Unocal shale oil production facilities located at Parachute, Colorado was distilled to produce the following distillates and residue: IBP-177°C (IBP-350°F, naphtha), 177-288°C (350-550°F, middle distillate), 288-427°C (550-800°F, atmospheric gas oil), 427-538°C (800-1000°F, vacuum gas oil), and 538°C+ (1000°F+) residue. Numerous chemical and physical properties were determined for this whole oil, its distillates and residue, and process intermediates. These analyses were conducted using either ASTM (ASTM 1985) or standard WRI procedures.

The middle distillate, atmospheric gas oil, and vacuum gas oil were selected for study because these distillates have potential for being converted into high-density aviation turbine fuel. The processes evaluated address those properties of the distillates that have to be modified to produce a turbine fuel: heteroatom and paraffin content, molecular weight, distillate range, and aromatic content.

Results

Table 1 shows the chemical and physical properties of the whole oil and the distillates that were evaluated with regard to the production of high-density aviation turbine fuel. The properties of the whole oil are typical of western shale oils, containing fairly high percentages of nitrogen and sulfur and having a specific gravity of about 0.9. The oil contained 11.8 wt % residue distilling above 538°C (1000°F).

Table 1. Chemical and Physical Properties of Western Shale Oil and Selected Distillates

Property	Whole Oil	Middle Distillate	Atmospheric Gas Oil	Vacuum Gas Oil
Elemental Composition, wt %				
Carbon	84.3	83.7	83.5	83.8
Hydrogen	12.0	13.2	13.0	12.4
Nitrogen	1.7	0.9	1.3	1.9
Sulfur	1.1	1.3	1.1	1.0
Oxygen[a]	0.9	0.9	1.1	0.9
Hydrogen-to-Carbon Atomic Ratio	1.70	1.88	1.86	1.76
Viscosity, cP 100°F	17.6	2.1	14.8	429
Specific Gravity, 60°F	0.9091	0.8430	0.9061	0.9530
Molecular Weight	320	210	270	390
Pour Point, °F	-	-56	57	100

[a] Oxygen determined directly, elemental composition then normalized to 100 wt %

As expected, the distillates and residue contain decreasing percentages of hydrogen and increasing percentages of nitrogen with increasing boiling range. Sulfur is evenly distributed across the distillate range, and oxygen is concentrated in the higher boiling distillates and residue. In addition, the specific gravity, viscosity, and molecular weight increase with increasing boiling point.

Since the application of the acid-base extraction, solvent dewaxing, and coking processes to the appropriate distillates did not produce intermediates that warranted further evaluation as fuel candidates, they will not be further discussed here. The application of Attapulgus clay treatment to selected distillates resulted in intermediates that were evaluated as potential fuel candidates. Test fuel #1 was prepared by passing the middle distillate through an Attapulgus clay column. Test fuel #2 was prepared by passing a 4 to 1 by volume mixture of the middle distillate and a 288-354°C (550-670°F) distillate through an Attapulgus clay column.

The chemical and physical properties of the fuel candidates are listed in Table 2. Test fuel #1 easily satisfies the hydrogen requirement of a high-density aviation turbine fuel. In addition, the amount of nitrogen is very low (39 ppm), the oxygen value is less than 0.1 wt %, and the distillation data meet the requirements of a high-density aviation turbine fuel. Also, the freeze point is only slightly above the required value of -47°C (-53°F). However, the sulfur content is too high (1.0 wt %), the specific gravity is too low (0.8180), and the net heat of combustion is too low (125,890 Btu/gal). To increase the specific gravity of the fuel candidate, a mixture was prepared containing 20 vol % of a higher boiling distillate. After clay treatment, the

specific gravity of test fuel #2 had increased from 0.8180 to 0.8259. Unfortunately, the increase was not enough to satisfy the high-density fuel requirement. In addition, the heteroatom content increased, and the freeze point increased dramatically to -25°C (-13°F). Because of the changes noted in the properties of the fuel candidates, we suspected that the paraffin content of the fuels was too high. The results of mass spectral analysis of the fuels proved this suspicion to be true. The mass spectral data show that the alkane content of test fuels #1 and #2 are 28.0 and 37.7 wt %, respectively. The requirement for a high-density fuel is less than 10 vol %. In addition, the aromatic content is also too high, 34.7 and 40.9 wt %, respectively. The requirement for this property is a maximum of 30 vol %.

Table 2. Chemical and Physical Properties of Fuel Candidates Prepared from Western Shale Oil

Property	High-Density Fuel	Test Fuel #1	Test Fuel #2
Elemental Composition, wt %			
Carbon	-	85.2	84.5
Hydrogen	13.0 min	13.8	14.0
Nitrogen	-	trace[a]	0.2
Sulfur	0.4 max	1.0	1.2
Oxygen[b]	-	<0.1	0.1
Specific Gravity, 60°F	0.850 min	0.8180	0.8259
Freeze Point, °F	-53 max	-45	-13
Net Heat of Combustion, Btu/gal	130,000 min	125,890	127,700

[a] Test Fuel #1 contained 39 ppm nitrogen
[b] Oxygen determined directly, elemental composition then normalized to 100 wt %

To reduce the heteroatom and aromatic content of the distillates, hydrogenation experiments were conducted using the middle distillate and atmospheric gas oil as the feeds to the reactor. Each distillate was hydrogenated at two different temperatures. This was done to determine the level of severity that is appropriate to convert the distillates to high-density turbine fuel intermediates. As expected, heteroatom content and distillate range of the intermediates significantly decreased with respect to the original distillates. The total heteroatom content was reduced from the 3.1- to 3.5-wt % level to the part-per-million level.

Hydrocarbon-group-type analysis of the process intermediates from the middle distillate shows that the amount of alkanes increased because of the partial saturation of alkenes. Consequently, the percentage of saturates in the process intermediates was only somewhat higher than that in the original distillate. However, the amount of aromatics in the process intermediates increased from 29 to about 37 wt %. This was due to an increase in the amount of monoaromatics (alkylbenzenes and indanes/tetralins). The process intermediates from the atmospheric gas oil also had an increase in alkanes. However, not only saturation of alkenes, but also

conversion of other classes of compounds through cracking resulted in this increase. Consequently, the percentage of saturates in these process intermediates increased from the 54 wt % originally present in the atmospheric gas oil to about 86 wt %. The amount of aromatics in the intermediates from the atmospheric gas oil decreased somewhat, exhibiting a shift from diaromatics to monoaromatics (alkylbenzenes and indanes/tetralins). Even though hydrogenation reduced the level of heteroatoms to the part-per-million level, the high concentration of alkanes in the process intermediates precluded their further evaluation as high-density aviation turbine fuels.

Conclusions

Several processes were evaluated for their ability to produce intermediates for the production of high-density aviation turbine fuel. These processes included acid-base extraction, solvent dewaxing, Attapulgus clay treatment, coking, and hydrogenation. Acid-base extraction and solvent dewaxing reduced the heteroatom and paraffin content of the distillates. In addition, coking reduced the distillate range, molecular weight, and specific gravity of the vacuum gas oil. However, none of these products was suitable for evaluation as fuel candidates because the heteroatom and paraffin contents of the products were too high.

Attapulgus clay treatment reduced the nitrogen and oxygen content of the middle distillate to the part-per-million level but the amount of sulfur, alkanes, and aromatics in the test fuels were higher than the target values established by the U.S. Air Force. In addition, the specific gravity and net heat of combustion of the test fuels were too low. Because acid-base extraction and Attapulgus clay treatment did not reduce the heteroatom content to the levels appropriate for a fuel candidate, hydrogenation was evaluated as a process to reduce heteroatoms and also to saturate the aromatic rings present in the middle distillate and atmospheric gas oil. The heteroatom content of the process intermediates was reduced to the part-per-million level. However, the amount of alkanes was too high to satisfy the requirements of a high-density aviation turbine fuel.

Because of the paraffinic nature of western shale oil, it appears that it will be quite difficult or expensive to prepare high-density aviation turbine fuel from this alternative fossil fuel.

Related Publications and Presentations

Publications

Thomas, K.P., and D.E. Hunter, 1989, The Evaluation of Western Shale Oil as a Feedstock for the Production of High-Density Aviation Turbine Fuel. Laramie, WY, DOE/MC/11076-2888.

Thomas, K.P., E.B. Smith, and D.E. Hunter, 1989, Advanced Fuels Research. Proceedings of the Ninth Annual Gasification and Gas Stream Cleanup Systems Contractors Review Meeting, Morgantown, WV, DOE/METC-89/6107, 282-291.

Presentations

Thomas, K.P., 1989, Advanced Fuels Research. Presented at the Ninth Annual Gasification and Gas Stream Cleanup Systems Contractors Review Meeting, Morgantown, WV.

Thomas, K.P., E.B. Smith, and D.E. Hunter, 1989, The Processing of Alternate Fossil Fuels to Produce High-Density Aviation Turbine Fuel. Presented at Confab '89, Laramie, WY.

EVALUATION OF PROCESSES FOR THE UTILIZATION OF EASTERN SHALE OIL AS A FEEDSTOCK FOR HIGH-DENSITY AVIATION TURBINE FUEL

Kenneth P. Thomas

Background

For many years, the U.S. Department of Defense and the U.S. Department of Energy have been involved in evaluating alternative fossil fuel sources as feedstocks for the production of conventional transportation fuels. For example, Sullivan and Frumkin (1986) studied conventional refining processes for the production of gasoline, diesel fuel, and jet fuel from coal-derived liquids. Moore et al. (1981) and Reif et al. (1982) evaluated various refining processes for the production of jet fuels from western shale oil. Other research sponsored by the U.S. Air Force investigated the conversion of tar sand bitumens and heavy crude oils to military jet fuels (Talbot et al. 1986; Moore et al. 1987). However, it appears that very little has been done to evaluate the process sequence and the properties of conventional transportation fuels produced from eastern shale oil.

With respect to the production of high-density aviation turbine fuel from shale oils, several papers have recently been published. For example, western shale oil was shown to not be a suitable feedstock for the production of high-density turbine fuel (Thomas and Hunter 1989a; Greene 1989). This is, primarily, because western shale oil is a very paraffinic fossil fuel. However, the only information that appears to be available concerning the evaluation of eastern shale oil as a feedstock for the production of high-density turbine fuel are the reports of Fahy and Vawter (1987) and Cha et al. (1989). They concluded that upon hydrogenation this very aromatic oil could make a good feedstock for the production of high-density aviation turbine fuel.

Objective

The objective of this study was to determine the feasibility of producing a high-density aviation turbine fuel from eastern shale oil.

Procedures

A sample of eastern shale oil was received from the Morgantown Energy Technology Center, Laramie Project Office. The oil was produced by Synfuels Engineering and Development Inc. (1989) using the Tosco II process. Normally, a routine analysis of the whole oil is made on the as-received sample. However, because of the very high solids and water content of the oil, a small portion of the oil was dissolved in toluene and then filtered to remove the solids. The water and toluene were removed from the resultant mixture by rotary evaporation. This sample constituted the "whole oil" for analysis. The distillates and residue and the subsequent process intermediates that were analyzed resulted from a rather laborious clean-up and distillation process (Thomas and Hunter 1989b). The shale oil resulting from this process was distilled to produce the following distillates and residue: IBP-177°C (IBP-350°F, naphtha), 177-288°C (350-550°F, middle distillate), 288-427°C (550-800°F, atmospheric gas oil), 427-538°C (800-1000°F, vacuum gas oil), and 538°C+ (1000°F+) residue. Numerous chemical and physical properties were determined for the whole oil, its distillates and residue, and process intermediates. These analyses were conducted using either ASTM (ASTM 1985) or standard WRI procedures.

The middle distillate, atmospheric gas oil, and vacuum gas oil were selected as the feed materials for process evaluation because these distillates have the potential of being converted into high-density

aviation turbine fuel. The processes that were evaluated included acid-base extraction, solvent dewaxing, Attapulgus clay treatment, coking, and hydrogenation. Acid-base extraction was used to reduce the heteroatom content of the middle distillate and atmospheric and vacuum gas oils. Solvent dewaxing was used to reduce the paraffin content of the atmospheric and vacuum gas oils. Attapulgus clay treatment was used to reduce the heteroatom content of the middle distillate. Coking was used to reduce the distillate range of the vacuum gas oil. Hydrogenation was used to reduce the heteroatom content and to saturate the aromatic rings in the middle distillate and atmospheric gas oil. These processes address the properties of the distillates that must be modified to produce a turbine fuel: heteroatom and paraffin content, molecular weight, distillate range, and aromatic content.

Results

The chemical and physical properties of the whole eastern shale oil and selected distillates are listed in Table 1. The data listed for the whole oil are for the oil after the solids and water were removed. An aliquot of the oil as delivered to WRI contained 17.9 wt % water, determined by azeotropic distillation with toluene, and 33.2 wt % solids, determined by filtration.

The whole oil is fairly aromatic, with a hydrogen-to-carbon (H/C) atomic ratio of 1.43, and contains modest amounts of nitrogen, sulfur, and oxygen. The specific gravity is 1.0178, reflecting its aromatic character. The viscosity and molecular weight of the whole oil are, respectively, 294 cP at 38°C (100°F) and 260 amu. The chemical and physical properties of this sample of eastern shale oil are comparable to other eastern shale oils produced by a

Table 1. Chemical and Physical Properties of Eastern Shale Oil and Selected Distillates

Property	Whole Oil	Middle Distillate	Atmospheric Gas Oil	Vacuum Gas Oil
Elemental Composition, wt %				
Carbon	84.0	85.1	85.1	85.7
Hydrogen	10.1	11.7	10.1	8.7
Nitrogen	2.0	0.7	1.6	2.0
Sulfur	1.6	1.2	1.7	1.9
Oxygen[a]	2.3	1.3	1.5	1.7
Hydrogen-to-Carbon Atomic Ratio	1.43	1.64	1.41	1.21
Viscosity, cP				
100°F	294	3.2	22.7	91,100
Specific Gravity,				
60°F	1.0178	0.8936	0.9690	1.0656
100°F	1.0040	-	0.9550	1.0518
Molecular Weight	260	200	250	380
Pour Point, °F	-	-35	14	77

[a] Oxygen determined directly, elemental composition then normalized to 100 wt %

variety of processes (Tokairin and Morita 1983; Ewert and Scinta 1983; Faulkner et al. 1983; Roberts et al. 1988). In general, the percentages of nitrogen, sulfur, and oxygen in the distillates and residue increase with increasing boiling range, while the H/C atomic ratio decreases with increasing boiling range. The viscosity, specific gravity, molecular weight, and pour point increase with increasing boiling range.

The process conditions and properties of the process intermediates are listed in Table 2. Evaluation of these results indicated that the products from acid-base extraction, solvent dewaxing, Attapulgus clay treatment, and coking were not suitable for further investigation as fuel candidates.

Table 2. Conditions Used and Properties of Process Intermediates Obtained from the Hydrogenation of Distillates from Eastern Shale Oil

	Middle Distillate		Atmospheric Gas Oil	
Process Conditions				
Pressure, psig	1500	1500	2000	2200
Liquid Hourly Space Velocity, V_o/V_c/hr	1	1	1	1
Hydrogen Feed, scfb	5000	5000	5000	6000
Temperature, °F	600	625	700	700
Hydrogen Consumption, scfb	800	918	1250	1105
Product Properties				
Elemental Composition,				
Carbon, wt %	87.2	87.2	88.4	88.2
Hydrogen, wt %	12.7	12.8	11.4	11.5
Nitrogen, ppm	1470	350	990	1610
Sulfur, ppm	104	46	620	1140
Specific Gravity, 60°F	0.9348	0.9318	0.9053	0.9118
Hydrocarbon Type, wt %				
Alkanes	16.8	14.4	28.0	30.5
Alkenes	10.8	13.3	20.7	19.5
Monocyclic Alkanes	3.1	6.6	6.3	5.6
Dicyclic Alkanes	0	0.3	0	0
Tricyclic Alkanes	1.6	1.1	0	0
Total Saturate Hydrocarbons	32.3	35.7	55.0	55.6
Alkylbenzenes	9.6	10.8	6.6	7.3
Indanes/Tetralins	54.4	52.0	31.8	26.9
Naphthalenes	3.7	1.5	0.9	1.8
Fluorenes	0	0	4.5	6.3
Anthracenes/Phenanthrenes	0	0	1.2	2.1
Total Aromatic Hydrocarbons	67.7	64.3	45.0	44.4

Since the processes tested to this point did not significantly improve the properties of the distillates, specifically the heteroatom and aromatic content, hydrogenation of the distillates was conducted. Each distillate was hydrogenated at two different sets of conditions. This was done to estimate the level of severity that might be appropriate for conversion of the distillates to high-density aviation turbine fuel intermediates.

As a result of the hydrogenation process, the heteroatom content of all intermediates significantly decreased with respect to the original distillates. Based on the results of hydrocarbon-group-type analysis, the process intermediates produced from the middle distillate contain less alkanes and alkenes than the original distillate. However, the percentage of monocyclic alkanes is increased. The result is that the percentage of saturates decreased from 50 to about 34 wt %. The percentage of monoaromatics (alkylbenzenes and indanes/tetralins) is increased with respect to the original distillate. This results in an increase in the aromatics from 45 to about 66 wt %. Of particular interest is that these process intermediates contain about 53 wt % indanes/tetralins, a component that upon further hydrogenation to dicyclic alkanes is important for the production of high-density turbine fuel. The process intermediates from the atmospheric gas oil have higher percentages of alkanes and monocyclic alkanes than the distillate. This results in an increase in saturates from 40 to about 55 wt %. The percentage of aromatics in the intermediates is increased from 36 to about 44 wt %. This increase in aromatics is the result of increased amounts of monoaromatics (primarily, indanes/tetralins). During the processing, diaromatics and triaromatics were lost. As observed for the intermediates from the middle distillate, the aromatics from the atmospheric gas oil were composed of, primarily, indanes/tetralins and some alkylbenzenes. Even though the hydrogenation process reduced the heteroatom content to about 0.1 wt % or less and the alkane content is fairly low (middle distillate intermediates contain about 15 wt % alkanes), the process intermediates were not suitable for further evaluation as a high-density turbine fuel. However, the high concentration of indanes/tetralins does suggest that eastern shale oil may be a suitable feedstock for the production of high-density aviation turbine fuel.

The middle distillate from eastern shale oil is composed of about 32 wt % indanes/tetralins. After a single-stage hydrogenation experiment, the percentage of this class of compounds is increased to about 53 wt %. In addition, the heteroatom content is reduced to about 0.1 wt % or less. It appears that a two-stage hydrogenation process may lead to the production of a high-density aviation turbine fuel from distillates of eastern shale oil. However, the first stage must be relatively mild for the removal of heteroatoms. The second stage is then more severe, for the saturation of alkenes and aromatic rings. If the conversion is not conducted using a two-staged approach, but rather a severe single-stage process, the result will be the opening of dicyclic structures to produce monocyclic structures (Thomas and Hunter 1989c).

Conclusions

Five processes were evaluated for their ability to produce intermediates from suitable distillates of eastern shale oil for the production of high-density aviation turbine fuel. The application of the acid-base extraction, solvent dewaxing, Attapulgus clay treatment, and coking processes did not result in intermediates that warranted further investigation as fuel candidates. Hydrogenation was evaluated as a process to not only reduce the heteroatom content, but also saturate the aromatic rings present in the middle distillate and atmospheric gas oil. The heteroatom content of the process intermediates was reduced to about 0.1 wt % or less. However, the saturation of aromatics and olefins was not accomplished during the application of the single-stage hydrogenation process. Consequently, evaluation of the process intermediates as fuel candidates was not conducted.

In summary, the processes evaluated did not produce materials that satisfied all of the requirements of a high-density aviation turbine fuel.

In spite of the difficulties in preparing fuel candidates suitable for evaluation as a high-density aviation turbine fuel, it is believed that a two-stage hydrogenation process can be employed to produce a high-density turbine fuel that would meet the requirements of the U.S. Air Force. This is based on the observation that the process intermediates from hydrogenation contain high concentrations of indanes/tetralins. Hydrogenation of indanes/tetralins to dicyclic alkanes results in a class of compounds that are necessary for the production of a high-density aviation turbine fuel.

Related Publication

Thomas, K.P., and D.E. Hunter, 1989, The Evaluation of Processes for the Utilization of Eastern Shale Oil as a Feedstock for the Production of High-Density Aviation Turbine Fuel. Laramie, WY, DOE/MC/11076-3023.

EVALUATION OF A COAL-DERIVED LIQUID AS A FEEDSTOCK FOR HIGH-DENSITY AVIATION TURBINE FUEL

Kenneth P. Thomas

Background

The conversion of coal-derived liquids to transportation fuels has been the subject of many studies sponsored by the U.S. Department of Energy and the U.S. Department of Defense. These studies evaluated conventional petroleum processes for the production of specification-grade fuels. For example, Sullivan et al. (1978) and Sullivan and Frumkin (1986) studied conventional refining processes for the production of transportation fuels from coal-derived liquids and western shale oil. Smith et al. (1988) evaluated the potential of producing conventional jet fuels from a by-product stream of the Great Plains Gasification Plant (Basin Electric). They concluded that the production of conventional military turbine fuels, JP-4 and JP-8, is possible but only through the use of large amounts of hydrogen, 3400 scfb. They also concluded that the production of a high-density aviation turbine fuel, JP-8X, is possible but only through special processing to satisfy specific gravity and freeze point requirements. As a continuation of the screening studies conducted by Smith et al. (1988), Furlong et al. (1989) evaluated various hydrogenation schemes to produce conventional jet fuels and high-density aviation turbine fuel from the tar oil (by-product) stream. They verified their process scheme, which includes three separate hydrogenation steps, by producing two barrels of JP-8 that met all of the military specifications, except the flash point. In addition, small quantities of JP-4 and JP-8X were produced. These products met all specifications except copper strip corrosion (JP-4 and JP-8X), heating value (JP-4), existent gum (JP-8X), and flash point (JP-8X). The copper strip corrosion and existent gum specifications probably would have been met if the samples had been clay-treated or if additives had been used. As a continuation of the study reported here, Greene et al. (1989) and Greene et al. (1990) evaluated various refinery processes to produce high-density aviation turbine fuel from coal-derived liquids. Employing a series of hydroprocessing steps, they produced fuels that exceed the net heating value requirement of a high-density aviation turbine fuel.

Objective

The purpose of this investigation was to determine the feasibility of producing a high-density aviation turbine fuel from a coal-derived liquid.

Procedures

A coal-derived liquid was received from the Morgantown Energy Technology Center. The liquid was produced by Coalite and Chemical Products Limited of England using a low-temperature carbonization process (Needham 1961). The liquid was distilled to produce IBP-177°C (IBP-350°F, naphtha), 177-288°C (350-550°F, middle distillate), 288-418°C (550-785°C, atmospheric gas oil), 418-538°C (785-1000°F, vacuum gas oil), and 538+°C (1000+°F) residue. No evidence of thermal cracking was observed during the distillations. Numerous chemical and physical properties were determined for the whole coal-derived liquid, its distillates and residue, and process intermediates. These analyses were conducted using either ASTM (1985) or standard WRI procedures.

The middle distillate, atmospheric gas oil, and vacuum gas oil were selected for process evaluation because these distillates have potential for being converted into high-density aviation turbine fuel. The processes that were evaluated included acid-base extraction, solvent dewaxing, Attapulgus clay treatment, coking, and hydrogenation. Acid-base extraction was used to reduce the heteroatom content of

the middle distillate and atmospheric and vacuum gas oils. Solvent dewaxing was used to reduce the paraffin content of the atmospheric and vacuum gas oils. Attapulgus clay treatment was used to reduce the heteroatom content of the middle distillate. Coking was used to reduce the distillate range of the vacuum gas oil, and hydrogenation was used to reduce the heteroatom content and to saturate the aromatic rings in the middle distillate and atmospheric gas oil. These processes address those properties of the distillates that must be modified to produce a turbine fuel: heteroatom and paraffin content, molecular weight, distillate range, and aromatic content.

Results

The chemical and physical properties of the whole coal-derived liquid and selected distillates are listed in Table 1. As is typical of coal-derived liquids, the whole oil is fairly aromatic, having a hydrogen-to-carbon ratio of 1.25. It also contains modest amounts of nitrogen and sulfur and a rather large amount of oxygen. The specific gravity is 1.0407, also reflecting its aromatic character, and the oil contains 8.7 wt % distilling above 538°C (1000°F). Nitrogen increases with increasing distillate range; while sulfur and oxygen are variable. The middle distillate has the highest amount of oxygen (7.3 wt %), probably phenols. As expected, the hydrogen-to-carbon ratio decreases with increasing distillate range, and the viscosity, specific gravity, molecular weight, and pour point increase with increasing distillate range. Note that the molecular weight of the vacuum gas oil was determined in pyridine rather than the customary solvent, toluene, because of the presence of preasphaltenes.

Table 1. Chemical and Physical Properties of a Coal-Derived Liquid and Selected Distillates

Property	Whole Oil	Middle Distillate	Atmospheric Gas Oil	Vacuum Gas Oil
Elemental Composition, wt %				
Carbon	82.9	82.2	85.2	85.0
Hydrogen	8.7	9.3	9.1	8.0
Nitrogen	1.1	0.5	1.1	1.4
Sulfur	1.1	0.7	0.8	1.0
Oxygen[a]	6.2	7.3	3.8	4.6
Hydrogen-to-Carbon Atomic Ratio	1.25	1.35	1.27	1.12
Viscosity, cP 100°F	67.8	42.0	83.2	97,800
Specific Gravity, 60°F	1.0407	0.9750	1.0313	1.1080
Molecular Weight	180	190	230	270[b]
Pour Point, °F	-	-29	57	97

[a] Oxygen determined directly, elemental composition then normalized to 100 wt %
[b] Molecular weight determined in pyridine, all other molecular weights determined in toluene

Unfortunately, acid-base extraction, solvent dewaxing, Attapulgus clay treatment, and coking did not produce intermediates that warranted further investigation as fuel candidates. In each case, the resulting intermediates contained too high of heteroatom and aromatic contents.

Consequently, hydrogenation experiments were conducted on the middle distillate and atmospheric gas oil with the goal being the removal of heteroatoms and the saturation of aromatic rings. The process conditions and properties of the process intermediates are listed in Table 2. Each distillate was hydrogenated at two different temperatures. This was done to estimate the level of severity that might be appropriate for conversion of the distillates to high-density aviation turbine fuel intermediates.

Table 2. Conditions Used and Properties of Process Intermediates from the Hydrogenation of Distillates from a Coal-Derived Liquid

	Middle Distillate		Atmospheric Gas Oil	
Process Conditions				
Pressure, psig	1750	1750	2000	2000
Liquid Hourly Space Velocity, V_o/V_c/hr	1	1	1	1
Hydrogen Feed, scfb	8000	8000	8000	8000
Temperature, °F	635	650	700	715
Hydrogen Consumption, scfb	2681	2835	2269	2559
Product Properties				
Elemental Composition,				
Carbon, wt %	86.0	85.9	87.8	87.6
Hydrogen, wt %	14.0	14.1	12.2	12.4
Nitrogen, ppm	<20	<20	270	59
Sulfur, ppm	<20	27	97	35
Specific Gravity, 60°F	0.9208	0.9178	0.9598	0.9558
Hydrocarbon Type, wt %				
Alkanes	4.2	3.8	8.8	13.7
Alkenes	34.2	35.1	17.5	17.4
Monocyclic Alkanes	34.2	36.2	18.5	17.8
Dicyclic Alkanes	0.6	1.4	1.8	1.1
Tricyclic Alkanes	0.5	0	0.2	0
Total Saturate Hydrocarbons	73.7	76.5	46.8	50.0
Alkylbenzenes	8.1	8.7	6.8	7.0
Indanes/Tetralins	18.0	14.7	42.8	40.7
Naphthalenes	0.2	0.1	0.8	0.8
Fluorenes	0	0	2.0	1.0
Anthracenes/Phenanthrenes	0	0	0.8	0.5
Total AromaticHydrocarbons	26.3	23.5	53.2	50.0

During the hydrogenation process, the heteroatom content of all intermediates significantly decreased with respect to the original distillates. The total heteroatom content was reduced from the 5.7- to 8.5-wt % level to the part-per-million level. In addition, a significant amount of thermal cracking occurred during the hydrogenation of the distillates. For the middle distillate, the conversion in distillate range was significant, the process intermediates contain about 50 wt % distilling below 177°C (350°F) rather than the original 3 wt %. For the atmospheric gas oil, a rather significant reduction in the distillate range also resulted because of the hydrogenation process. More than one-third of the material distilling in the 288-427°C (550-800°F) range was converted to the next lower reported distillate range. The specific gravity of the process intermediates was decreased with respect to the original distillates. The specific gravity of the distillates ranged from 0.9750 to 1.0313, whereas the specific gravity of the process intermediates ranged from 0.9178 to 0.9598.

Hydrocarbon-group-type analysis of the process intermediates produced from the middle distillate contained less alkanes than the original distillate. However, the percentage of alkenes in the intermediates doubled because of the processing. Monocyclic alkanes were also significantly increased. The percentage of saturates increased from 40 to about 75 wt %. The percentage of aromatics remained about the same as that in the original distillate. The aromatics were composed of, primarily, indanes/tetralins and some alkylbenzenes. The process intermediates from the atmospheric gas oil contained about the same amount of alkanes and three times the amount of alkenes as the original distillate. In addition, they contained significant amounts of monocyclic alkanes. The percentage of saturates increased from 19.7 to about 48 wt %. The percentage of aromatics also increased, in this case, from 38.1 to about 52 wt %. As observed for the intermediates from the middle distillate, the aromatics from the atmospheric gas oil were composed of, primarily, indanes/tetralins and some alkylbenzenes. Even though the hydrogenation process reduced the heteroatom content to the part-per-million level and the alkane content was low, the intermediates were not suitable for evaluation as high-density turbine fuels because their alkene contents were too high and, for those intermediates from the atmospheric gas oil, the aromatic contents were too high. However, the high concentration of indanes/tetralins does seem to suggest that this coal-derived liquid may be a suitable feedstock for the production of high-density aviation turbine fuel.

The hydrogenation studies reported here parallel those of Smith et al. (1988). The combined results of the two studies demonstrate that during the hydrogenation of a coal-derived liquid containing high concentrations of heteroatoms, in particular oxygen, the reactions occur in the following order: sulfur removal, oxygen removal, and nitrogen removal and ring opening. Saturation of double bonds competes with these processes and results in products that are either partially hydrogenated or reflect ring-opening reactions. If these results are compared with earlier work (Smith et al. 1986) on FCC light cycle oil and pyrolysis fuel oil, there is almost complete conversion of naphthalene to dicyclic alkanes. However, the higher ring-number structures are not exclusively converted to their saturate analogs. These structures also undergo ring opening and alkyl chain cleavage to yield tetralin-type structures. It appears that two-stage hydrogenation is necessary, but the first stage must be relatively mild with the goal being the removal of heteroatoms, in particular oxygen. The second stage is then more severe, with the goal being the saturation of alkenes and aromatic rings. If the processing is not conducted using this two-stage approach, a single-stage process will result in the opening of one of the rings of the dicyclic structures to produce monocyclic structures.

Conclusions

Five processes were evaluated for their ability to produce intermediates from suitable distillates for the production of high-density aviation turbine fuel. Acid-base extraction, solvent dewaxing, Attapulgus clay treatment, and coking resulted in products that contained high concentrations of heteroatom- and aromatic-containing structures. Consequently, further evaluation of these products was not warranted.

Hydrogenation was evaluated as a process to not only reduce the heteroatom content, but also saturate the aromatic rings present in the middle distillate and atmospheric gas oil. The heteroatom content of the process intermediates was reduced to the part-per-million level. However, the saturation of aromatics and olefins was not accomplished during the application of the single-stage hydrogenation process. Consequently, evaluation of the process intermediates as fuel candidates was not conducted. In summary, the processes evaluated did not result in the production of materials that satisfied all of the requirements of a high-density aviation turbine fuel.

Despite the difficulties in preparing fuel candidates suitable for evaluation as high-density aviation turbine fuels, it is believed that a two-stage hydrogenation process can be employed to produce a high-density turbine fuel that would meet the requirements of the U.S. Air Force. This premise is based on the observation that the process intermediates from hydrogenation contain high concentrations of dicyclic alkanes and indanes/tetralins, compounds that are necessary for the production of a high-density aviation turbine fuel.

Related Publications and Presentation

Publications

Thomas, K.P., and D.E. Hunter, 1990, Advanced Fuels Research: The Evaluation of a Coal-Derived Liquid as a Feedstock for the Production of High-Density Aviation Turbine Fuel. Proceedings of the Tenth Annual Gasification and Gas Stream Cleanup Systems Contractors Review Meeting, Morgantown, WV, DOE/METC-90/6115, 490-499.

Thomas, K.P., and D.E. Hunter, 1989, The Evaluation of a Coal-Derived Liquid as a Feedstock for the Production of High-Density Aviation Turbine Fuel. Laramie, WY, DOE/MC/11076-2993.

Presentation

Thomas, K.P., and D.E. Hunter, 1990, Advanced Fuels Research: The Evaluation of a Coal-Derived Liquid as a Feedstock for the Production of High-Density Aviation Turbine Fuel. Presented at the Tenth Annual Gasification and Gas Stream Cleanup Systems Contractors Review Meeting, Morgantown, WV.

ADVANCED FUELS RESEARCH REFERENCES

ASTM, 1985, Annual Book of ASTM Standards. American Society for Testing and Materials, Philadelphia, PA.

Cha, C.Y., F.D. Guffey, and L.J. Fahy, 1989, Development of Recycle Oil Pyrolysis and Extraction Process for Recovering Oil from Eastern Oil Shale. Proceedings, 1988 Eastern Oil Shale Symposium, Institute for Mining and Minerals Research, Lexington, KY, IMMR 88/101, 301-313.

Ewert, W.M., and J. Scinta, 1983, Hydrogen Retorting of Indiana Shale in a Loop Reactor System. Synthetic Fuels from Oil Shale and Tar Sands, Institute of Gas Technology, Chicago, IL, 395-406.

Fahy, L.J., and R.G. Vawter, 1987, Horizontal Low-Void Retorting of Eastern and Western Shale. Proceedings, 1986 Eastern Oil Shale Symposium, Kentucky Energy Cabinet Laboratory, Lexington, KY, KECL 86-158, 141-149.

Faulkner, B.P., M.H. Weinecke, and R.F. Cnare, 1983, The Allis-Chalmers Roller Grate Retort Process for Eastern Shale. Synthetic Fuels from Oil Shale and Tar Sands, Institute of Gas Technology, Chicago, IL, 545-561.

Furlong, M., J. Fox, and J. Masin, 1989, Production of Jet Fuels from Coal Derived Liquids, Vol IX--Results of Bench-Scale and Pilot Plant Testing. Air Force Aero Propulsion Laboratory, Wright-Patterson Air Force Base, OH, Air Force Report AFWAL-TR-87-2042.

Greene, M., 1989, Lummus Crest Inc. monthly report prepared for the U.S. Department of Energy dated June 14, 1989, Report No. 25020-08, Contract No. DE-AC21-88MC25020.

Greene, M., S. Huang, V. Strangio, and J. Reilly, 1989, High Energy Density Military Fuels by Hydroprocessing of Coal Pyrolyzates. ACS Division of Fuel Chemistry Preprints, 34(4): 1197-1205.

Greene, M., S. Huang, and J. Masin, 1990, High Energy Density Turbine Fuels from Mild Coal Gasification Liquids. Proceedings of the Tenth Annual Gasification and Gas Stream Cleanup Systems Contractors Review Meeting, Morgantown, WV, DOE/METC-90/6115, 384-393.

Moore, H.F., L.M. Henton, C.A. Johnson, and D.A. Fabry, 1981, Refining of Military Jet Fuels from Shale Oil: Part II. Air Force Aero Propulsion Laboratory, Wright-Patterson Air Force Base, OH, Air Force Report AFWAL-TR-81-2056.

Moore, H.F., C.A. Johnson, D.A. Fabry, and M.H. Chaffin, 1987, Aviation Turbine Fuels from Tar Sands Bitumen and Heavy Oils: Part II. Air Force Aero Propulsion Laboratory, Wright-Patterson Air Force Base, OH, Air Force Report AFWAL-TR-84-2070, Part II.

Needham, C.E., 1961, Reactive Fuels and Chemicals from Coal. Institute of Petroleum Review, 15(174): 165-171.

Reif, H.E., J.P. Schwedock, and A. Schneider, 1982, An Exploratory Research and Development Program Leading to Specifications for Aviation Turbine Fuel from Whole Crude Shale Oil: Part IV. Air Force Aero Propulsion Laboratory, Wright-Patterson Air Force Base, OH, Air Force Report AFWAL-TR-81-2087.

Roberts, M.J., D.M. Rue, and W.C.S. Hu, 1988, Synthesis Gas Retorting of Eastern Oil Shales. Proceedings, 1987 Eastern Oil Shale Symposium, Kentucky Energy Cabinet Laboratory, Lexington, KY, KECL 87-175, 333-341.

Smith, E.B., F.D. Guffey, and L.G. Nickerson, 1986, Evaluation of High-Density Fuels Derived from Light Pyrolysis Fuel Oil or Light Cycle Oil. Report prepared for Geo-Centers, Inc., Newton Upper Falls, MA, Contract No. F337615-84-C-2412, Subcontract No. 416-006.

Smith, E.B., F.D. Guffey, and L.G. Nickerson, 1988, Production of Jet Fuels from Coal Derived Liquids, Vol III--Jet Fuels Potential of Liquid By-Products from the Great Plains Gasification Project. Air Force Aero Propulsion Laboratory, Wright-Patterson Air Force Base, OH, Air Force Report AFWAL-TR-87-2042.

Sullivan, R.J., B.E. Strangeland, C.E. Ruby, D.C. Green, and H.A. Frumkin, 1978, Refining and Upgrading of Synfuels from Coal and Oil Shales by Advanced Catalytic Processes, First Interim Report, Processing of Paraho Shale Oil. DOE Report HCP/T2315-25.

Sullivan, R.J., and H.A. Frumkin, 1986, Refining Coal Liquids: Where We Stand. ACS Division of Fuel Chemistry Preprints, 31(2): 325-339.

Synfuels Engineering and Development, Inc., 1989, Eastern Oil Shale Research Involving the Generation of Retorted and Combusted Oil Shale Waste, Shale Oil Collection, and Process Stream Sampling and Characterization. Rifle, CO, DOE/MC/24092-2725.

Talbot, A.F., V. Elanchenny, J.P. Schwedock, and J.R. Swesey, 1986, Turbine Fuels from Tar Sands Bitumen and Heavy Oil, Phase II: Laboratory Sample Production. Air Force Aero Propulsion Laboratory, Wright-Patterson Air Force Base, OH, Air Force Report AFWAL-TR-85-2013, Part II.

Thomas, K.P., and D.E. Hunter, 1989a, The Evaluation of Western Shale Oil as a Feedstock for the Production of High-Density Aviation Turbine Fuel. Laramie, WY, DOE/MC/11076-2888.

Thomas, K.P., and D.E. Hunter, 1989b, The Evaluation of Processes for the Utilization of Eastern Shale Oil as a Feedstock for the Production of High-Density Aviation Turbine Fuel. Laramie, WY, DOE/MC/11076-3023.

Thomas, K.P., and D.E. Hunter, 1989c, The Evaluation of a Coal-Derived Liquid as a Feedstock for the Production of High-Density Aviation Turbine Fuel. Laramie, WY, WRI-91-R009.

Tokairin, H., and S. Morita, 1983, Properties and Characterizations of Fischer-Assay-Retorted Oils from Major World Deposits. Synthetic Fuels from Oil Shale and Tar Sands, Institute of Gas Technology, Chicago, IL, 247-265.